NSWC/WOL/TR 75-163 27 February 1976

SCATTERING OF ELECTROMAGNETIC RADIATION BY APERTURES: IX. SURFACE CURRENT DISTRIBUTION OVER A CLOSED CYLINDRICAL CAN AT BROADSIDE INCIDENCE.

This report contains essentially experimental results of research into an electromagnetic diffraction problem. The study was performed jointly in the Physics Department at the State University of New York in Albany, N.Y., and at the Naval Surface Weapons Center /White Oak. At the Naval Surface Weapons Center, White Oak these efforts were supported partly by the Defense Nuclear Agency under Task DNA-EB088-52 and partly by the Independent Research Program (Task Number MAT-03L-000/ZR011-01-01). At the State University of New York the effort was partially supported by NSWC/WOL under contract N60921-75-C-0131. This document is for information only.

LEMMUEL L. HILL

TABLE OF CONTENTS

LIST OF FIGURES

LIST OF FIGURES (Contd.)

I. INTRODUCTION

This report presents the experimentally obtained distribution of surface current components on the end caps and sidewall of a conducting circular cylinder of finite length L and radius a. A monochromatic, linearly polarized, plane electromagnetic wave is assumed irradiating the capped cylinder at broadside incidence in a direction normal to the cylinder axis. Data has been taken for the two independent cases of E-polarization in which the electric field in the incident radiation is polarized parallel to the axis of the cylinder, and of H-polarization where the incident electric field is polarized perpendicular to the cylinder axis. The frequencies of the incident radiation used during the studies were chosen so as to constrain the circumference to wavelength ratio, γ, as well as the length to wavelength ratio, L/λ, to lie in the so called resonance region. That is to say, neither ratio is very large nor very small. Figure 1 illustrates the geometry.

Before proceeding it is probably helpful to pause momentarily and explain the role of this paper in our series of publications on the effects of apertures on the scattering characteristics of conducting systems. Clearly a completely closed conducting can has no apertures. However, since we are studying the intrinsic effects of apertures in systems we must first establish, for reference, the diffraction characteristics of these systems in the absence of such

apertures. Thus, for example, we shall be issuing a sequence of reports on the effects of a variety of apertures in finite conducting cylinders. Obviously it is essential to know what changes they generate in the physical response of the same finite cylinder in the absence of apertures.

Returning to our introduction to the problem of the diffracting closed cylindrical can we next review the history of the problem. Perhaps the first development was the reduction of the problem by Maue[1] who derived the general formulation of the coupled integral equations for the fields on the surface of a completely closed perfect conductor. These are the often used and sometimes sadly abused E-field and H-field integral equations. Maue included some guiding consideration of the case where the conducting surface contained sharp edges. Unfortunately, he left explicit solution of the simultaneous coupled integral equations, except for the infinite cylinder, to those who would follow him. Hönl, Maue and Westpfahl[2] repeated and expanded the discussion of the earlier Maue formal investigation into scattering of electromagnetic radiation by a closed perfectly conducting target. Van Bladel[3] also derived the pure integral equation for the surface current on an irradiated

---

1. A. W. Maue, "Zur Formulierung eines Allgemeinen Beugungsproblems durch eine Integralgleichung," Zeitschrift für Physik 601, 126 (1949).
2. H. Hönl, A. W. Maue, K. Westpfahl, "Theorie der Beugung," Vol. XXV/1 pp. 311, 354-362, Handbuch der Physik, Springer-Verlag, Berlin, 1961.
3. J. Van Bladel, "Electromagnetic Fields," p. 354, McGraw-Hill Book Co., N.Y., 1964.

closed perfect conductor. There are pros and cons associated with the integral equation approaches to the solution of the scattering problem for a perfectly conducting finite target. The surface integral equation has the advantage of recasting a three dimensional problem into one that is intrinsically two-dimensional in form. On the other hand this has the disadvantage of leading to an equation which is very difficult to solve formally. Thus far no one has succeeded in obtaining an analytic solution in closed form for the particular diffraction problem that is the subject of this report.

Any attempt at analytic resolution of the scattering problem of a finite conducting circular cylindrical can with flat end caps must not fail to consider several very important points. First of all there are sharp edges where the flat end caps join the side wall. The general problem of edge conditions has been examined in considerable detail by Bouwkamp[4], Meixner[5,6], Jones[7] and Heins and Silver[8]. For a discussion of this edge problem see the excellent reference book by Jones[9] or the solution,in the vicinity of an edge, given in

---

4. C. J. Bouwkamp, "A Note on Singularities At Sharp Edges In Electromagnetic Theory," Physica, 467-474, 12 (1946).
5. J. Meixner, Die Kantenbedingung in der Theorie der Beugung Electromagnetisher Wellen an Vollkommen Leitenden Ebenen Schirmen," Ann. Physik, 2-9, 441 (1949).
6. J. Meixner, "The Behaviour of Electromagnetic Fields at Edges," N.Y.U. Inst. Math, Sci. Res. Rept. EM-72, December 1954.
7. D. S. Jones, "Note on Diffraction by An Edge," Quart. J. Mech. and Appl. Math 420, 3 (1950).
8. A. E. Heins, S. Silver, "The Edge Condition and Field Representation Theorems In the Theory of Electromagnetic Diffraction," Proc. Camb. Phil. Soc. 149, 51 (1955).
9. D. S. Jones, Section 9.1, "The Theory of Electromagnetism," MacMillan Co., New York, N.Y. 1964.

terms of Bessel functions by Collins.[10] These discussions, such as that by Collins, are strictly true for the two dimensional conducting wedge. For such a right angle wedge the field components tangent to the edge vanish at the edge. Since the surface current component directed normal to that edge is related to the tangential component of magnetic field parallel to that edge it vanishes at the edge. Field components normal to the edge and hence the tangential component of current parallel to the edge go as $R^{-1/3}$ (where R is the distance to the edge) as the edge is approached. These results, it is believed, should also apply to edges occurring in three-dimensional problems. This is presumably the consequence in the two-dimensional case of the singular behaviour of the fields near the edge being determined by only the currents and charges in the immediate vicinity. From this point of view a short segment of a curved edge appears to be much the same as the edge of a two-dimensional system. This presumed behaviour in three-dimensions can be compared to the actual currents detected as the edge is approached along the curved sidewall and also along the flat end caps. Analytic solutions via numerical form using the high speed computers have considerable difficulty in faithfully predicting such special analytic singular type behaviour. Another possible source of error that can inadvertently enter in attempts to obtain the numerical solution with computers is just as serious and requires some comment at this point. Since we are solving an exterior problem we must take care to identify extraneous

10. R. E. Collins, F. J. Zucker, Section 1.7, "Antenna Theory" Part I, McGraw-Hill Book Co., New York, N.Y. 1969.

contributions of interior modes when using the computer output. In analytic abstract attempts at solving the exterior problem one normally just omits all interior solutions as they should not enter the problem. This is not so conveniently managed when obtaining numerical resolution of the problem from the computer. Extremely useful discussions of this difficulty have been presented by Greenspan and Werner,[11] and Garabedian.[12] Methods to help avoid such errors have been proposed by a number of investigators.[13-21] This difficulty, inherent in the use of the high speed computer to

---

11. D. Greenspan, P. Werner, "A Numerical Method for The Exterior Dirichlet Problem for the Reduced Wave Equation," Arch. Ration. Mech. Anal., 288, 23 (1966).
12. P. R. Garabedian, "An Integral Equation Governing Electromagnetic Waves," Quart. Appl. Math., 428, 12 (1955).
13. P. C. Waterman, "Matrix Formulation of Electromagnetic Scattering," Proc. IEEE, 805, 53, Aug 1965.
14. H. A. Schenk, "Improved Integral Equation Formulation For Acoustic Radiation Problem," Acoust. Soc. Am., 41, 44 (1968).
15. K. M. Mitzner, "Numerical Solution of the Exterior Scattering Problem at Eigen Frequencies of The Interior Problem," 1968, U.R.S.I. Meeting, Boston, Mass. March 1968.
16. H. Brakhage, P. Werner, "Über des Dirichletsche Aussenraumproblem für die Helmholtzsche Schwingungsgleichung," Arch. Math. Chapter 16, pp. 325-329 (1965).
17. J. C. Bolomey, W. Tabbara, "Numerical Aspects on Coupling Between Complementary Boundary Value Problems," IEEE Trans. on Ant. and Propag. 356, AP-21 (1973).
18. J. C. Bolomey, W. Tabbara, "Sur la Resolution Numerique de l'Equation des Ondes pour des Problemes Complementaires," C. R. Acad. Sci. (Paris), 933, 271B (1970).
19. J. C. Bolomey, W. Tabbara, "Influence du Mode de Representation de l'Onde Diffractee Sur la Resolution Numerique d'un Probleme de Diffraction," C. R. Acad. Sci. (Paris), 1001, 270B (1970).
20. J. C. Bolomey, These d'Etat Université de Paris XI, Paris, France May 1971.
21. R. F. Kussmaul and P. Werner, "Fehlerabschätzungen für ein Nümerisches Verfahren zur Auflösung Linearer Integralgleichungen mit Schwachsingulärer Kerner," Comput. Jour. 22, 3 (1968).

obtain solutions of diffraction by closed targets, is still not completely resolved and consequently considerable caution must be exercised in interpreting computer solutions and attempting to compare them with experimental data.

VanVleck, Bloch, and Hammermesh[22] performed one of the earliest investigations of the scattering by a circular cylindrical can with flat end caps. In their approximation study the interest was centered on radar back scattering. Actually the point of departure for their study was an earlier result established in an earlier study of Bloch and Hammermesh.[23] They had obtained results that showed a thin antenna of arbitrary cross-sectional shape has much the same far-field electromagnetic characteristics as a solid right circular cylinder of the same length but with an equivalent radius a_e. As an example of their results they found that for a flat strip the equivalent radius is one-fourth the width of the strip. In the VanVleck paper the radar targets are referred to as "wires" and are assumed to be circular cylinders to be consistent with the context of the Bloch-Hammermesh work. VanVleck's group recognized immediately that in the design of their radar reflectors it was of importance to know the response of the wire as a function of its length and radius and also the radar wavelength. They observed that for a given wavelength of

22. J. H. VanVleck, F. Bloch, M. Hammermesh, "Theory of Radar Reflection from Wires and Thin Metallic Strips," Jour. Appl. Phys. 274, 18 (1947).
23. F. Bloch, M. Hammermesh, Technical Memo 411-125 of the Radio Research Laboratory, Harvard University, Cambridge, Mass., June 20, 1944.

the incident radiation there is an optimum length for back-scattering. In addition they noted that there is a band of frequencies for each wire diameter which corresponds to a strong response from the target. Radar back-scattering by wires involves most of the pertinent features of antennas and presents a good opportunity for comparing predictions of theory with measurements which can be made under controlled laboratory conditions. Calculating the current induced in the wire by the incident radiation constituted the initial step VanVleck had to take to solve the wire back-scattering problem. Siegel and Labus[24] had developed a simple method for handling similar problems. In their technique, known as the "e.m.f. method," a reasonable assumption is made for the form of the current expression. Then requiring that energy be strictly conserved the current expression is numerically evaluated. This is definitely not a method for rigorously deducing the solution to the antenna problem. VanVleck's group followed a different more rigorous method. They tried to satisfy the Maxwell equations and to fulfill the boundary conditions at the wire surface. This required using a method of successive approximations. The wire was assumed to be a perfect conductor. Thus the total tangential electric field, incident plus that induced by the current in the wire, must vanish on the surface of the wire. They assumed the wires and hence the solid cylinders were sufficiently thin so that the currents at the ends could be assumed zero. Mathematically speaking all of these statements are equivalent to an integral equation that

24. E. Siegal, J. Labus, Hoch: tech. und Elek:akus., 166, 43 (1934).

must be solved. Hallén[25-27] proposed a method of successive approximation for the integral equation and using this technique King and Harrison[28-30] solved the integral for the thin wire receiving antenna. Unfortunately even for the thin wire the original Hallén method is inadequate for the wire length equal to or larger than the incident wavelength. Gray[31] and King and Middleton[32] overcame this difficulty by devising different procedures of successive approximation. Middleton and King [33] have published a critique of the various schemes proposed for approximate solution of the antenna integral equation. The VanVleck method is essentially that of King, and Middleton. Although the thin wire antenna theory has a history of successfully predicting the radiation fields far from the source it

---

25. E. Hallén, "Theoretical Investigations into the Transmitting and Receiving Qualities of Antennae," Nova Acta Reg. Soc. Scient. Upsaliensis, 1, 11, (1938).
26. E. Hallén, "Exact Treatment of Current Wave Reflection at the End of a Tube Shaped Cylindrical Antenna," I.R.E. Trans. on Ant. and Propag. 479, AP-4 (1956).
27. E. Hallén, "Exact Solution of the Antenna Equation," Electromagnetic Theory and Antennas, Ed. E. C. Jordan, Pergamon Press, New York, p. 1131, 1963.
28. R. King, C. W. Harrison, Jr., "The Distribution of Current Along A Symmetrical Center-Driven Antenna," Proc. I.R.E. 548, 31 (1943).
29. R. King, C. W. Harrison, Jr., "The Receiving Antenna," Proceedings of I.R.E., 18, 32 (1944).
30. R. King, C. W. Harrison, Jr., "The Receiving Antenna In a Plane-Polarized Field of Arbitrary Orientation," Proc. I.R.E. 35, 32 (1944).
31. M. C. Gray, "A Modification of Halléns Solution of the Antenna Problem," Jour. Appl. Phys. 61, 15 (1944).
32. R. King, D. Middleton, "The Cylindrical Antenna: Current and Impedance," Quart. Appl. Math, 302, 3 (1946).
33. D. Middleton, R. King, "The Thin Cylindrical Antenna: A Comparison of Theories," Jour. Appl. Phys. 273, 17 (1946).

is still a limiting case problem where the wire radius is quite small compared to the wavelength of the radiation in question. Furthermore the near fields at the wire, as predicted by the theory, are still not accurate. We shall not discuss the VanVleck work any further since we are really concerned with closed cylinders whose radii are comparable in length to the wavelength. Kieburtz[34] also attempted a high-frequency asymptotic solution of the scattering by a flat capped, finite, conducting circular cylinder. In his problem he considered the special case of an arbitrarily oriented cylinder of very small radius and finite length. This is basically the same problem VanVleck attacked. Kieburz used a spatial Fourier transform of the tangential electric field. He then constructed the transform on the infinite extension of the cylinder by employing the boundary conditions at the cylinder ends and at large distances from it. His solution contains the normal mode-traveling waves along with the continuous part resulting from a branch cut integration. Only the circularly symmetric wave (TEM) was considered by Kieburz. This necessarily limited the solution to small radius cylinders. Unfortunately Kieburz did not publish any numerical results for his solution. We are including the thin finite length wire solutions in this discussion solely as a possible result which may serve as something to which we may be able to compare our results. It should be borne in mind, however, that in the thin wire problem the ends are assumed open so that in fact the circular hollow tube is being

34. R. B. Kieburz, "Scattering by a Finite Cylinder," Electromagnetic Waves, Ed. E.C. Jordan, Pergamon Press, New York, p. 145, 1963.

considered. Generally it has been assumed that for the thin wire there is no real difference between the solid cylinder and the hollow tube. A number of other simplifying assumptions which lead to agreement between far field theory and far field measurements are made for the thin wire. These have as a consequence the effect of making thin wire current distributions of very little practical value for comparison with the fat, closed, circular can current distributions. Other workers have extended the Bloch, Hammermesh[23] idea of treating thin wires of non circular cross-section by finding equivalent wires of circular cross-section with appropriate effective radii. To cite a few we mention the outstanding worth of Flammer,[35] Su and German,[36] and Uda and Mushiake.[37] Since these are thin wire studies they are similarly restricted in their utility for comparing results with the fat closed circular can.

Another line of approach to the finite length circular cross-section conducting cylinder is worth mentioning. This is via variational methods. The earliest such work appears to be that of Tai.[38,39] Unfortunately this attempt was again in the limit of the thin wire. Nevertheless the method is one of importance.

---

23. F. Bloch, M. Hammermesh, Ibid.
35. C. Flammer, "Equivalent Radii of Thin Cylindrical Antennas With Arbitrary Cross Sections," Stanford Research Inst. Tech. Rep. 4, 1950, Stanford, Calif.
36. C. W. H. Su, J. P. German, "The Equivalent Radius of Noncircular Antennas," Microwave Jour. 64, 9 (1966).
37. S. Uda, Y. Mushiake, Yagi-Uda Antenna, Sasaki Printing and Publishing Co. Ltd., Sendai, Japan 1954.
38. C. T. Tai, "Radar Response From Thin Wires," Stanford Res. Inst. Tech. Rep. 18, Stanford, Calif. 1951.
39. C. T. Tai, "Electromagnetic Back-Scattering From Cylindrical Wires," Jour. Appl. Phys. 909, 23 (1952).

Many other theoretical attempts have been made in the thin wire limit. Since the results are more pertinent to the general problem of the hollow finite length circular tube we shall defer referencing them. A subsequent report on the hollow tube problem will contain an extensive detailed discussion of these other works.

A rather illuminating aspect of the problem of diffraction by the closed can is contained in a discussion of the radar back-scattering cross-section by such a system. This discussion was that of Barrick[40] in a two volume radar cross-section handbook compiled by the Battelle Memorial Institute of Columbus, Ohio. This handbook summarizes the state of the art up to about the year 1970. The handbook states that when both the cylinder length and cylinder radius are comparable to the wavelength there appears to be no valid approximation for computing the scattered field. Resort to measured far field data was suggested as the only means to obtain valid results. Carswell[41] did determine, experimentally, the back-scattered cross-section from a finite cylinder for H-polarized incident radiation from end-on to broadside incidence. In his experiments he chose the fixed value of circumference to wavelength ratio $\gamma=0.72$ but allowed the length to wavelength ratio to range from 0.230 to 1.01. Radar back-scattering cross-section measurements, in principle, can be used by invoking "inverse scattering theory" to

---

40. G. T. Ruck, D. E. Barrick, W. D. Stuart, C. K. Krichbaum, "Radar Cross-Section Handbook," Vol. 1, Plenum Press, N.Y. Section 4.3.2.2, 1970.
41. A. I. Carswell, "Microwave Scattering Measurements in the Rayleigh Region Using a Focused-Beam System," Canad. Jour. of Phys. 1962, 43 (1965).

yield the surface currents on the target. Unfortunately the development of the "inverse problem" has not evolved to the extent that makes it a reliable tool.

Andrews[42] made some near field measurements of the diffracted fields near very thin, half-wave long conducting circular cylindrical rods. Although the data is useful it was limited by the existing probes used in the measurements at that time. An interesting semi-empirical study of the diffraction of electromagnetic radiation by a finite length solid circular metallic cylinder was carried out by Lind.[43] Although this work is not well known it is a very promising one. Lind's work is an approximation at arbitrary oblique incidence that employs the dominant n=o, TEM propagating mode for a conducting infinite cylinder. A reflection coefficient was defined for the ends of the cylinder and then experimentally determined for different diameter cylinders. Although the effects at the ends have been played down somewhat since they are not too important in the far field the method is still a significant one. The approximate semi-empirical method can in fact be improved upon to give a reasonably good prediction of the near fields and surface currents. Once this is done the semi-empirical predictions can be compared with our measured results and probably will result in further improvement in the theory.

---

42. C. L. Andrews, "Diffraction of Microwaves Near Rods," Jour. Appl. Phys. 465, 22 (1951).
43. A. C. Lind, "Resonance Electromagnetic Scattering by Finite Circular Cylinders," PhD. Dissertation, Rensselaer Polytechnic Institute, Troy, New York 1966.

At present heavy reliance is being placed on computer programs to numerically resolve the finite length, closed can near field problem. Harrington and Mautz[44] have devoted considerable effort to this end. Thus far, however, they have published results only for thin cylinders with radii on the order of a few percent of the wavelength and lengths comparable to the wavelength. Richmond[45] has made outstanding contributions in the use of the computer for many complex electromagnetic problems. So far it appears that he has only published results for a hollow thin wire open at the ends.

To help provide some guidance to the many people attempting to solve the problem of the near fields of a diffracting finite length, fat circular metallic can with flat end caps we have carried out a systematic experimental program. This program has taken advantage of detectors that are reliable and quite small (and introduce thereby minimal perturbations) to obtain the surface current distribution on the side wall and the end caps. In the next section we discuss the experimental techniques utilized. This is then followed by a presentation of the measured results. Finally some discussion of the results are presented.

---

44. R. F. Harrington, J. R. Mautz, "Straight Wires With Arbitrary Excitation and Loading," IEEE Trans. on Antennas and Prop., 502, AP15 (1967).
45. J. H. Richmond, "Digital Computer Solutions of the Rigorous Equations for Scattering Problems," Proc. of IEEE, 796, 53 (1965).

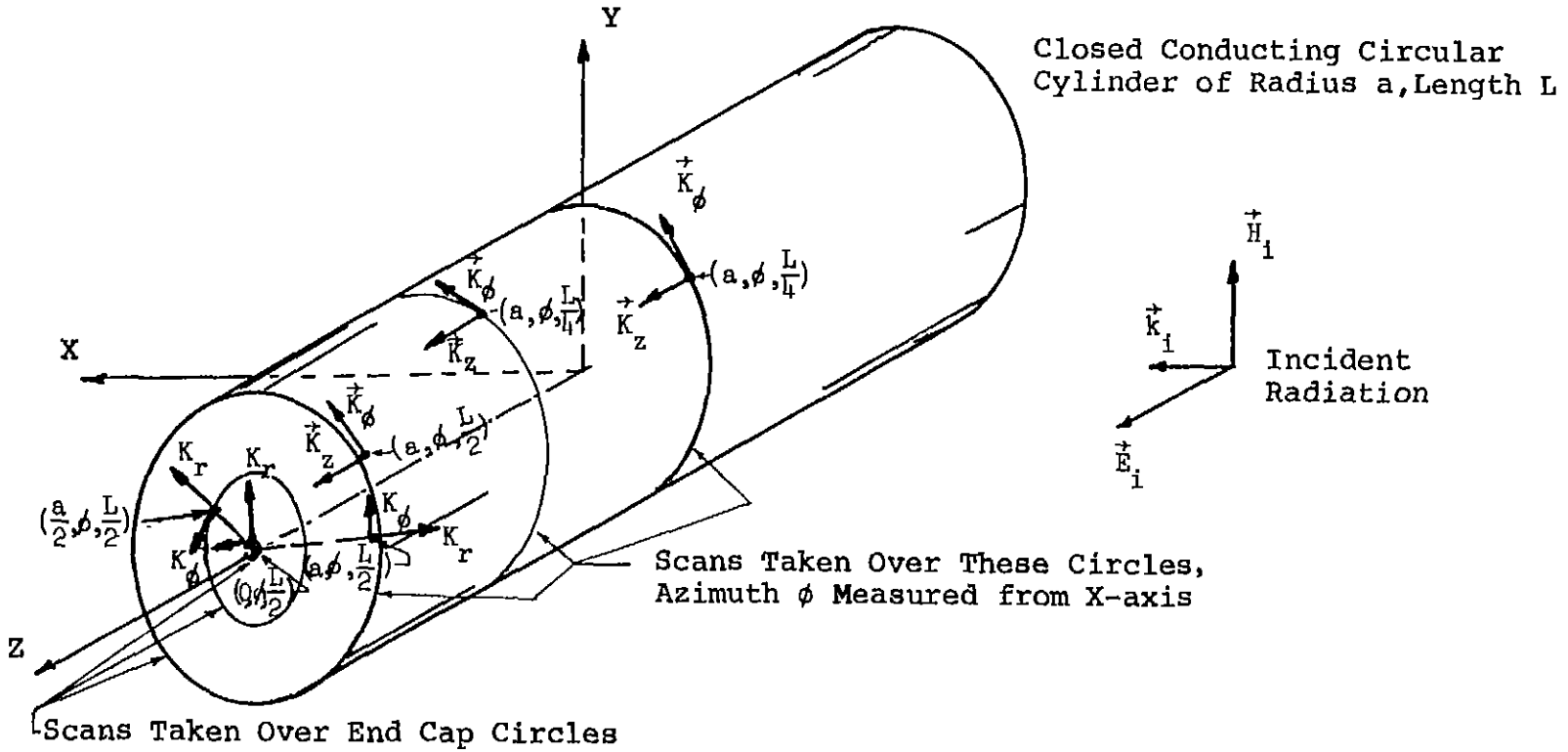

Figure 1. Geometry for Surface Current Components, $\vec{K}_j$, Scanned On A Completely Closed Finite Circular Cylinder Irradiated Broadside.

II. EXPERIMENTAL TECHNIQUE

All measurements were made utilizing the tapered anechoic chamber shown schematically in figure 2. The advantages of using a tapered anechoic chamber have been discussed elsewhere[46] and hence we omit any detailed consideration of this topic here. As indicated in figure 2 the source, located at the small end of the chamber, was a short section of L-band wave guide and is essentially a point source. In figure 3 we present a block diagram of the circuits. The power delivered to the source was obtained from a General Radio Signal Generator, Type 1218-B, Unit Oscillator, 900-2000 MHz, with a minimum of 300 milliwatts output over the complete frequency range. The output from a magnetic field detector of the target surface was fed to a Princeton Applied Research Lock-In Amplifier, Model JB-4. This amplifier provided a 4000 MHz modulation to a Scott, Decade amplifier Type 140A and thence to the General Radio Oscillator. Since all of these components are standard shelf items their characteristics can be obtained directly from the corresponding company manuals and we shall not go into any further discussion of them.

In the measurements presented here we have taken advantage of a unique feature that characterizes the magnetic field sensors used. This singular property results in data superior in accuracy to

---

46. R. Dell, C. Carpenter and C. L. Andrews, Jour. Opt. Soc. of Am. 62, 902 (1972).

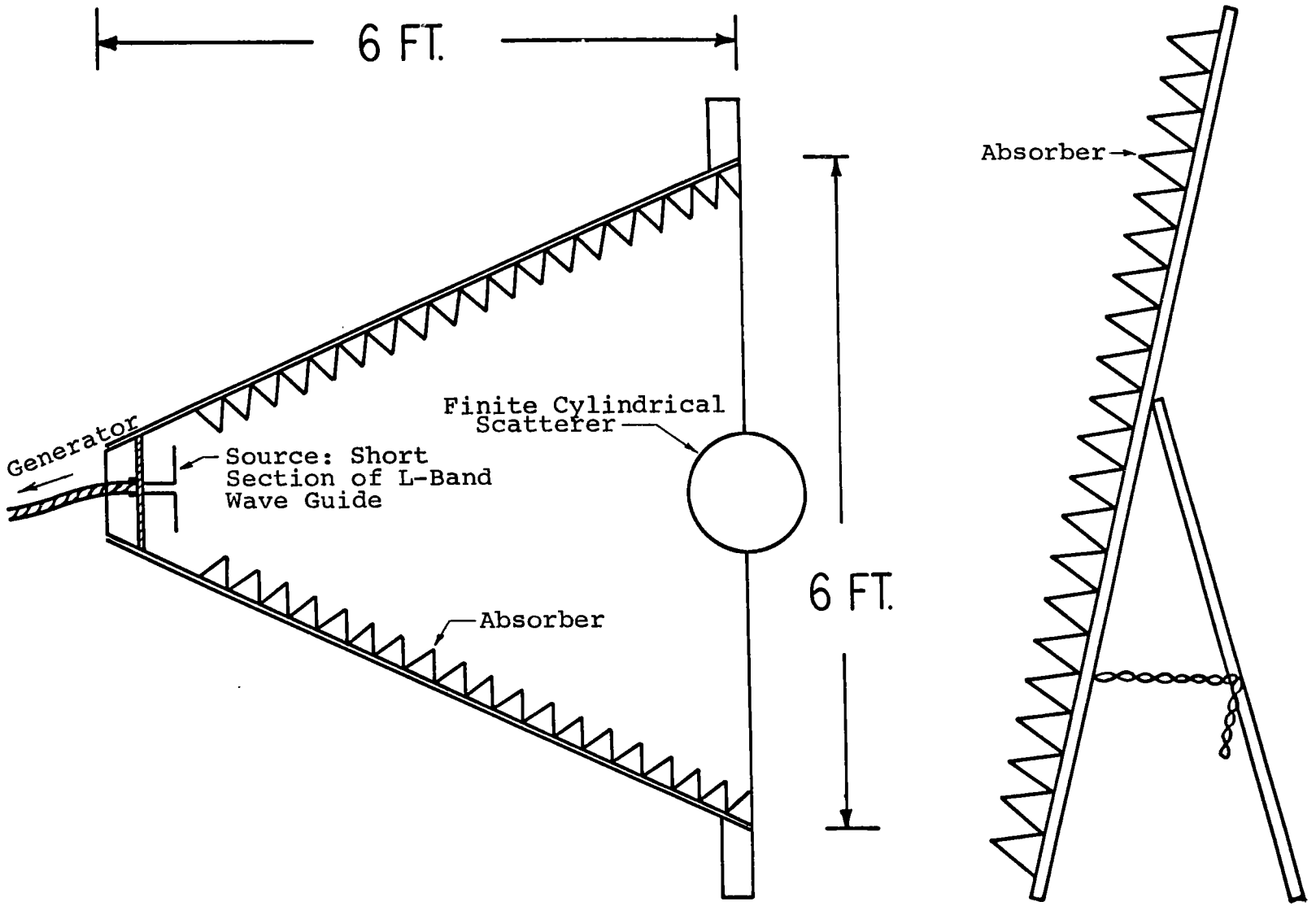

Figure 2 Schematic Layout of Tapered Anechoic Chamber Used for Measurements

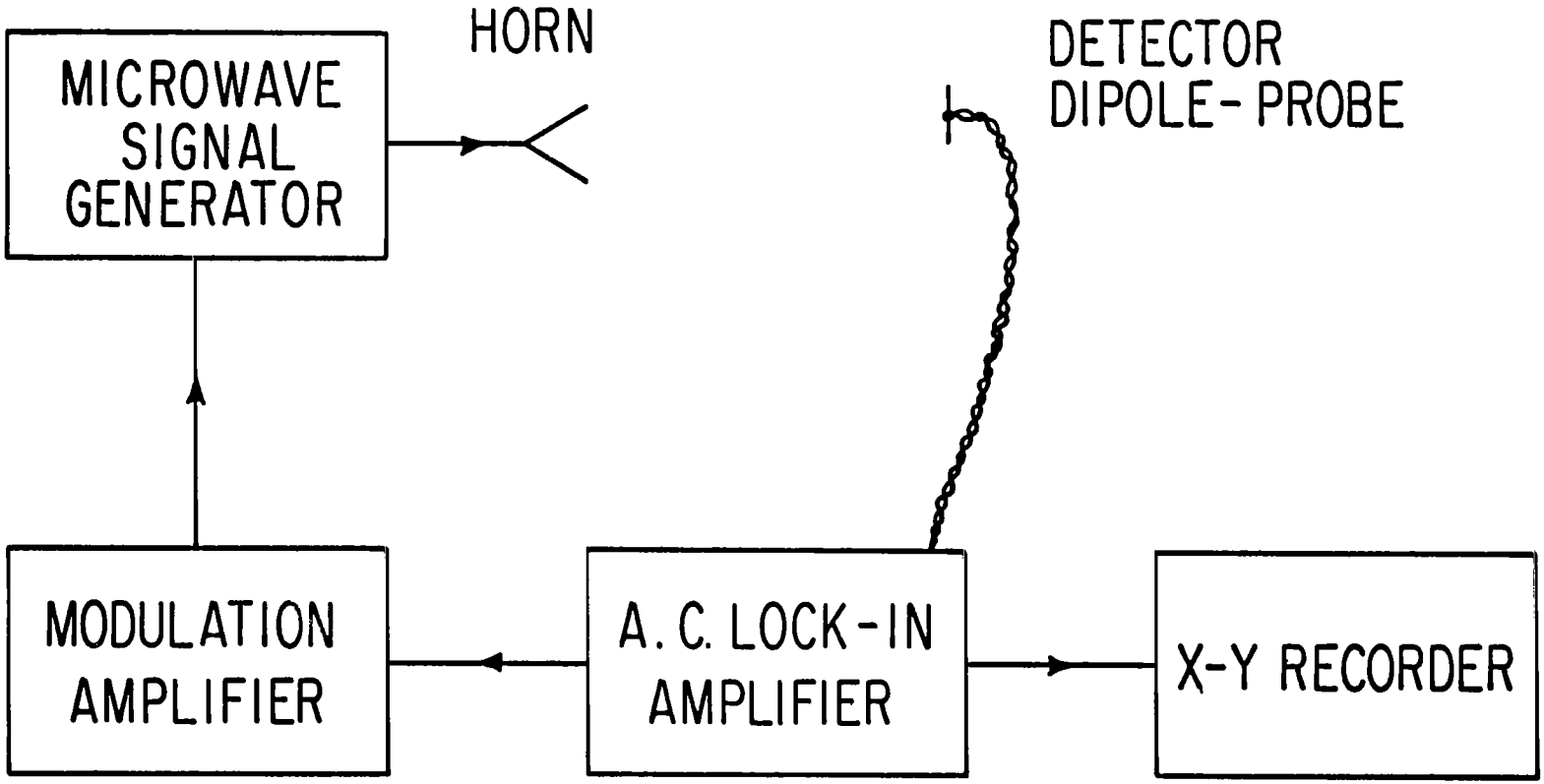

Figure 3 Block Diagram of Circuits Used for Diffraction Measurements and Recording Results

similar measurements performed earlier.[47-49] The remarkable feature of the sensor is its physical size. In figure 4 we illustrate diagramatically the small magnetic loop detector. The loop probe is mounted as shown on a precision ground alumina block for reliable repeatability. For the gold loop the dimensions were 0.30 cm in the direction normal to the surface of the cylinder and 0.40 cm parallel to the surface of the cylinder. Located on the top of the alumina block is an encapsulated Schottky diode. As can be seen in the diagram there is a 0.010 inch gap in the gold loop just at the bottom of the alumina block. Associated with this gap is sufficient capacitance at microwave frequencies to complete the circuit. To the ends of the gold leaf loop, at the gap, tungsten wires were attached. These wires were 0.6 cm in length and 0.0003 inches in diameter. These wires were fine enough to eliminate any significant perturbation of the microwave field. Thus the microwave circuit is just the loop antenna itself. When visually examining the probe the tungsten wires appear to merely resemble fine hairs. The precisely machined alumina block bearing the gold leaf loop antenna with the fine tungsten wires attached was cemented with clear epoxy to a base consisting of a thin sheet of alumina. This is also clearly discernible in figure 4. As may also be seen in this figure the tungsten wires have attached to them twisted leads of 0.003 inch

47. L. F. Libelo, J. P. Heckl, C. L. Andrews, D. P. Margolis, 1975 IEEE International EMC Symposium, October 1975, San Antonio, Texas. Paper No. 5BI.
48. D. P. Margolis, Ph.D. Dissertation, State University of New York at Albany. Albany, N.Y. January 1976.
49. D. P. Margolis, C. L. Andrews, R. L. Kligman, L. F. Libelo, Bull. Amer. Phys. Soc., 456, 19 April 1974.

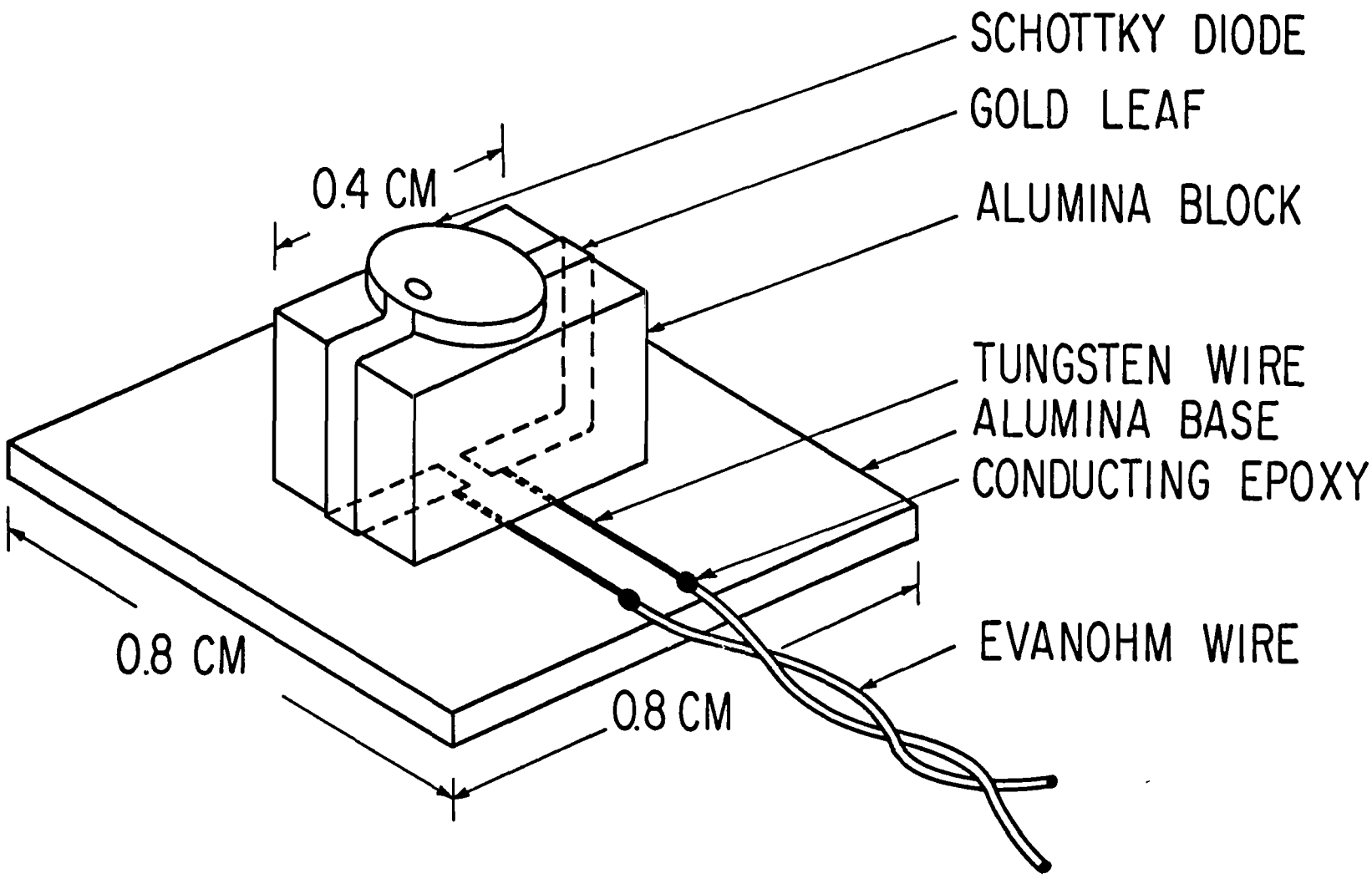

Figure 4 Diagram of the Magnetic Field Sensor

diameter high resistance enameled Evanohm wire. Conducting epoxy was used to attach these twisted leads. The Evanohm leads conduct the modulated, rectified potential difference to the Lock-in Amplifier. Taking advantage of the fact that the output power of the General Radio source was higher than the power levels used in our earlier measurements together with the fact that we are working in a shorter length anechoic chamber we obtained intensity levels at the conducting cylindrical target adequate for us to use the new small probes for measurements. Over the range of frequencies reported on here the height of the loop ranges from 0.01 to 0.02 wavelengths. For such a range of relative sizes measurements very close to the surface of a scatterer are accurate to within 2 to 3%. This is probably a conservative estimate. Mounting the target as shown in figure 5 enabled us to take azimuthal scans around the can.

In subsequent reports of results obtained in the presence of apertures in the finite metallic can we shall more fully elaborate on the experimental aspects.

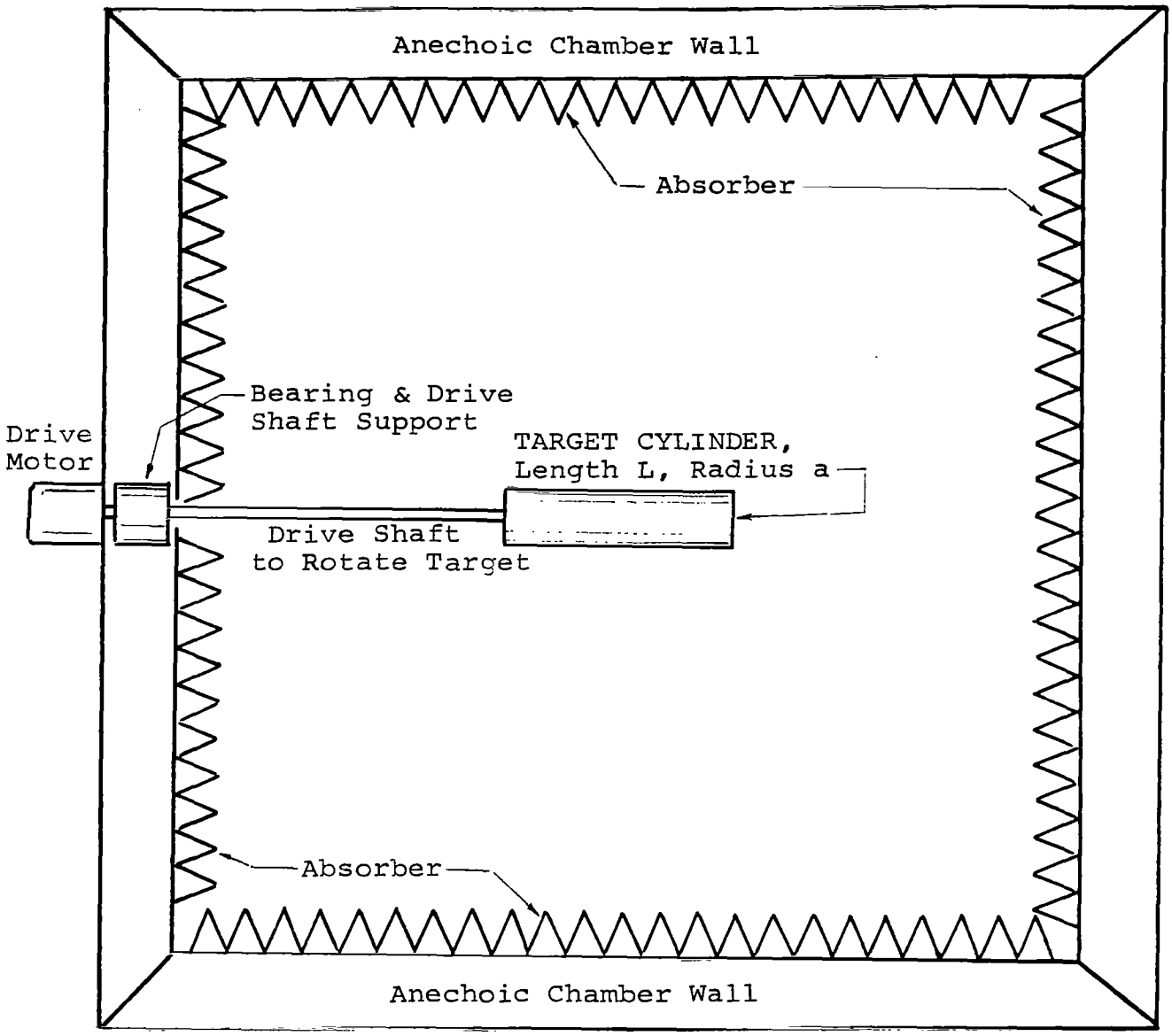

Figure 5. End View of Chamber Looking Toward Source Showing Rotatable Target Cylinder

III. RESULTS OF MEASUREMENT

Measurements of the surface currents were made in the manner described in the previous section. The diffracting object was a hollow, thin walled, circular metallic cylinder of fixed length L=46cm, closed at each end by a flat circular metallic cap of fixed radius a=5.10cm. By changing the frequency of the incident linearly polarized monochromatic plane electromagnetic wave and repeating the measurements we can obtain the frequency or wavelength dependence, for each polarization, of the induced current distribution over the capped metallic can. Results are presented in this report only for frequencies ranging from 1 GHz to 2 GHz in steps of 0.2 GHz. This gives rise to a largest length to wavelength ratio just twice the smallest value of this ratio. The same is true of the circumference to wavelength ratio. Table 1 below presents these parameters in a highly visible form.

Table 1. Length to Wavelength and Circumference to Wavelength Ratios for the Length L=46cm, and Radius a=5.10cm Diffracting Cylinder.

Frequency GHz	Wavelength λ(cm)	Length/Wavelength L/λ	Circumference/Wavelength $\gamma=2\pi a/\lambda$
1.0	30.0	1.53	1.068
1.2	25.0	1.84	1.281
1.4	21.5	2.14	1.490
1.6	18.8	2.44	1.704
1.8	16.7	2.77	1.918
2.0	15.0	3.07	2.136

For each frequency or wavelength in Table 1 we experimentally scanned from $\phi=0°$ to $\phi=360°$ each component of surface current for E-polarized and also for H-polarized broadside incident radiation. By symmetry considerations we observe that the scan from $\phi=0°$ to $\phi=180°$ coincides with the distribution from $\phi=0°$ to $\phi= -180°$ hence the results need be plotted for only half the range of azimuth ϕ. This holds on the end caps as well as on the sidewall. Experimentally it was observed that the current amplitudes were even functions of the longitudinal coordinate Z. This fact together with the observation that for a given polarization of the incident radiation only one current component is non-vanishing around the center of the cylinder yields some very significant information concerning the properties of the formal analytic solution of the closed-can diffraction problem. By appropriate application of this empirically derived information the formal solution of the problem is considerably simplified. For computer solution of the diffraction problem this is of no mean significance. In a subsequent report on formal solution of the flat capped cylinder we shall go into this point in considerable detail. We shall merely note here that in view of the experimental results we need only give the measured currents for the cylinder from Z=0 to Z= $\frac{1}{2}$L. Azimuthal scans were made at the center of the cylinder side wall i.e. Z=0. For E-polarization and again for H-polarization of the incident radiation the azimuthal distribution was obtained for the longitudinal component and the azimuthal component of the surface current. This was repeated at least for each frequency listed in Table 1. It is a simple matter

to determine whether the scan is actually around the center of the sidewall and the source, target and detector are properly aligned. This is achieved when only the one appropriate current component is determined to be non-vanishing and simultaneously the scan from $\phi=0°$ to $\phi=180°$ is indentical to that from $\phi=360°$ to $\phi=180°$. Although this is a simple procedure in principle in actual practice it is time consuming and quite a tedious affair to accomplish proper positioning and alignment. It should be noted that the experiment actually measures the amplitude of a component of magnetic field, per unit amplitude of incident magnetic field, very close to the metallic surface. Since the probe size to wavelength ratio is about 1/30 to 1/60 the measured magnetic field amplitudes are those at the surface to within a very few percent of error. It is well known that a magnetic field component at the surface of a perfect conductor is equal to the component of surface current, at that same point, normal to the magnetic field. Hence we are in fact obtaining quite precisely the amplitudes of surface current components. Leaving the special case of the Z=0 current component scans momentarily we point out that scans were made on the sidewall at other non-central values of Z. Again the question of proper alignment occurs. This time however we also have to correctly position the probes with respect to longitudinal distance from the cylinder centerline. By performing scans and adjusting orientation of source, target and detector until we have the appropriate symmetry in azimuth and a repeat of the angular distributions for both the axial and the azimuthal current components we can at least establish that we are

scanning correctly at the same distance on either side of center. At this stage we can determine that distance by simple measurement to lightly inscribed circles over which the scans were finally matched up so to as have coincident results. Again the technique is a quite simple one in principle but time consuming in practice. Clearly it is a somewhat tedious task to correctly scan at pre-selected distances from the centerline of the finite length cylinder. Nevertheless, we have carried out such scans and show below the results obtained. Amplitudes of the longitudinal component and the azimuthal component of surface current were measured around the sidewall at $Z=\frac{1}{4}L$ i.e. one-half the distance from center of the cylinder to the end of the can. Scans at the ends of the sidewall were made also. For these the outer gold leaf on the probe was positioned 7mm from the end of the cylinder to obtain $|K_z(\phi)|=|H_\phi(\phi)|$ i.e. the longitudinal component of current very close to the end of the cylinder. For the scans of $|K_\phi(\phi)|=|H_z(\phi)|$ the probe was positioned so as to have the gold-leaf and Schottky-diode loop in from the end about 2mm. The locations of the sensors should be kept in mind when the corresponding experimental data is examined. Scans of the radial current amplitude and the azimuthal current amplitude were made on the flat end caps also. Similar care must be exercised in properly locating and orienting the source, target and detector for the end cap measurements. As anticipated this is a somewhat more delicate procedure than on the sidewall of the can as only one endcap is available for the scans. The radial component of current near the edge of the cap was scanned by positioning the loop so that

the outermost side was fixed 7mm from the edge and the top path, containing the Schottky diode, was aligned to lie along a radius from the center of the end cap. To obtain scans of the azimuthal components of surface current on the end cap near its outer edge, the detector was aligned perpendicular to a radius of the end cap. This was done simultaneously with the outside edges of the vertical parts of the gold leaf loop about 2mm in from the edge of the cap. After properly locating and aligning the detector both components of current were scanned, azimuthally, halfway between the center and edge of the flat conducting end cap. Finally because of the finite size of the detector and other physical limiting factors it was virtually impossible to obtain the scans at the very center of the end cap. It is interesting to note that at the precise center only a radial component of current or equivalently only an azimuthal component of magnetic field must, in principle, exist. This renders it rather difficult to measure such physical quantities. Scans of the components of surface current were obtained by correctly positioning the detector slightly off center on the cap. These scans were made with the loop centered about 2mm from the end cap center. Once again we repeat that the positions of the probes during the scans must be kept in mind when considering the experimental results below. Although we are never precisely at an edge or exactly on the center point of the end cap our probes are nevertheless quite small physically and we are probably as close to these locations as is now possible to be. At least no one else has managed to get in as close as we have thus far.

An extremely important feature of the measurement program is to establish the actual value of $|H_j|/|H_o|$. The technique for calibrating the detectors will be briefly discussed now. For the ideal case of normal incidence on an infinite, circular, conducting cylinder the analytic solutions are well known.[50-53] Thus $|H_j|^2/|H_o|^2$ is known for the infinite cylinder. It should be recalled that for the infinite cylinder only one component of magnetic field is non-vanishing namely the component parallel to the incident magnetic field. This characteristic is also true around the center of a finite cylinder. It follows from symmetry arguments and was verified experimentally. Consider the point $(\gamma,\phi,z)\equiv(a,o,o)$. This is the center of a finite length conducting cylinder on the side away from the source i.e. the shadow side. For H-polarization the measured value $|H_z|/|H_o|$ at (a,o,o) for a cylinder of length 46cm was the same as that obtained at the same point for a cylinder of length 120cm using the same detector in the same incident field. Thus we can normalize this experimental result to the corresponding value of $|H_z|/|H_o|$ for the infinite cylinder of the same radius. This then calibrates the probe for the given wavelength and the true value of all other magnetic field measurements at that wavelength can be

---

50. J. J. Bowman, T.B.A. Senior and P.L.E. Uslenghi, eds., "Electromagnetic and Acoustic Scattering by Simple Shapes," Chapt. 2, North Holland Publishing Co, Amsterdam, The Netherlands 1969.
51. R. F. Harrington, "Time Harmonic Electromagnetic Fields," p.232-234 McGraw-Hill Book Co., New York 1961.
52. M. Kerker, "The Scattering of Light and Other Electromagnetic Radiation," Chapt. 6, Academic Press, New York 1969.
53. R.W.P. King, T.T. Wu, "The Scattering and Diffraction of Waves," Harvard Univ. Press, Cambridge, Mass. 1959.

determined for our finite cylinder. Repeating this procedure we can obtain the actual value of the measured magnetic fields over the range of frequency in Table 1. Now we have established all our measurements reported here to be the actual amplitude of the magnetic field components per unit amplitude incident magnetic field or equivalently we have the true amplitudes of the surface current components per unit amplitude incident magnetic field. We next turn our attention to the experimental results themselves.

Experimentally we observed that around the center line of the flat end capped metallic cylinder only one component of surface current was induced at normal broadside incidence. This was true for all frequencies. For E-polarized incident radiation only a longitudinal current component, K_z, or azimuthal magnetic field H_ϕ exists for z=o whereas for H-polarized incident radiation field only an azimuthal current component K_ϕ or longitudinal magnetic field H_z exists around the z=o line on the cylinder. As shall be discussed in a subsequent report this fact together with other symmetry displayed by the measurements lead to a considerable simplification of the analytic approach to solving this problem. Figures 6 and 12 show respectively the current amplitude distributions around the center of the cylinder for the frequencies of Table 1 for E-polarized and H-polarized incident radiation. It should be noted that the overall qualitative behaviour displayed by the measured currents in these figures for z=o corresponds quite closely to the current distributions of an infinite cylinder of the same radius. There is a clear pronounced maximum at $\phi=180°$, on the side facing the source, a much less pronounced minimum at about $\phi=45°$ on the shadow side, and

a small maximum at $\phi=o^{o}$ itself. Note, however, in figure 12 that for H-polarization and $\gamma=2.136$ we find more structural detail in the angular distribution of the current. This behaviour is also found for the corresponding infinite cylinder at $\gamma=2.136$. Consider next figures 7 and 13 which show respectively the experimental results at E-polarization and H-polarization for scans made at $z=\frac{1}{4}L$, halfway between the center of the cylinder and its flat-capped edge. Bear in mind that we are now about 0.4λ away from the edge for the longest wavelength and about three quarters of a wavelength from the edge for the smallest wavelength. In the E-polarization case we observe a number of interesting results. First the azimuthal component of surface current is about two orders of magnitude smaller than the z-component of current and was undetectable with our experimental method. Second the distribution of $|K_z|$ for the smallest wavelength ($\gamma=2.136$) is pretty much the same as at the centerline i.e. for $z=o$. On the other hand there is a marked variation in the relative amplitudes for the longest wavelength ($\gamma=1.068$) as we go from $z=o$ to $z=\frac{1}{4}L$. It is probably safe to assume then that for E-polarization one can use with reasonable accuracy the theoretical infinite cylinder results, for that portion of the finite cylinder corresponding to $-\frac{1}{4}L \lesssim z \lesssim \frac{1}{4}L$ for $L/\lambda \approx 3$ and, simultaneously $\gamma \approx 2$. Further the fact that K_ϕ is neglible out to $z \approx \frac{1}{4}L$ for E-polarization for the smaller circumference to wavelength ratios, γ implies that any computer approach may also be significantly improved upon. However, one will still have to account for the non-negligible variation in K_z over this portion of the cylinder. It is helpful to note that the non-

vanishing dominant component of surface current out to $z \approx \frac{1}{4}L$ still displays the qualitative characteristics of the distribution for the infinite cylinder surface current even for the smaller γ. In the H-polarization case we see from figure 13 that we have a somewhat different situation. To begin with the longitudinal component of surface current is detectable at $z=\frac{1}{4}L$ and was found to be about an order of magnitude smaller than the azimuthal component of surface current. As expected $|K_z|$ has minima at $\phi=0°$ and 180° just where $|K_\phi|$ has maxima. Note also that for the shortest wavelength case $\gamma=2.136$ we find $|K_z|$ also has maxima at about $\phi=45°$ and $\phi=120°$ which is just about where $|K_\phi|$ has minima for $\gamma=2.136$. It is interesting to observe in figure 13 that both $|K_\phi|$ and $|K_z|$ exhibit a minimum at about $\phi=90°$ for $\gamma=2.136$. The remaining scans for the different γ's show similar occurrences of maxima and minima in $|K_z|$ and $|K_\phi|$. Except for $\gamma=1.704$ the azimuthal scans at z=o and $z=\frac{1}{4}L$ of $|K_\phi|$ seem to be about the same for H-polarization. We see in figure 13 that at $z=\frac{1}{4}L$ for $\gamma=1.704$ the current $|K_z|$ exhibits the greatest relative change in amplitude as the azimuth varies from the shadow side at $\phi=o°$ to the illuminated side at $\phi=180°$. It should be noted that even though the amplitude of $|K_z|$ or $|H_\phi|$ is quite small, for H-pol, at $z=\frac{1}{4}L$ we were still able to detect some rather fine detail in the azimuthal scans. Clearly we have not exhausted all the information displayed in figures 6, 7, 12 and 13. We have probably just skimmed the surface. Nevertheless, a considerable amount of light has already been shed on the problem in our rather brief discussion so far.

Let us continue to move along the sidewall of the closed cylinder until we are in the vicinity of the edge i.e. $z \approx \frac{1}{2}L$. The measured results are shown in figure 8 for E-polarization and figure 14 for H-polarization. Consider the E-polarization case first. We find now that the current component $|K_\phi|$ that had been quite small and negligible out to $z \approx \frac{1}{4}L$ is now not only measurable, in detail, but is in fact quite appreciable in amplitude. Again we observe that $|K_\phi|$ has maxima where $|K_z|$ has minima and vice versa. What we are observing near the end of the cylinder is the strong manifestation of the results of a number of simultaneously occurring physical properties. Recall that we are considering incident radiation polarized parallel to the rotational symmetry axis of the can. On the side wall this produces the dominant longitudinal current of the center which only slowly damps out until near the very end where it falls very sharply to zero at z=L/2 since it is a current component normal to an edge. Indeed the precipitous manner at which it must drop to zero can be best appreciated by considering at $\phi=180°$ the case for $\gamma=1.704$. For this value of circumference to wavelength ratio $|K_z|^2/|H_o|^2$ is about maximum at z=o and drops off to a minimum at $z=\frac{1}{4}L$ of about one-half the maximum value at the center. Very close to the end of the cylinder $|K_z|^2$ has recovered its maximum amplitude and must then drop to zero over the remaining short distance to the edge. While this is taking place the azimuthal component of current, $|K_\phi|$, is only very slowly increasing from being identically zero at z=o. Since this is a component of current that becomes singular at the very end of the cylinder we find that it must be rising very rapidly over a

rather small distance from the cylinder edge. Hence the appreciable value of the amplitude scans of $|K_\phi|$ detected near the end of the cylinder and shown in figure 8. It should be recalled that for E-polarization the electric field in the incident wave is normal to the edges of the cylinder and the physical implications of this are apparent in the experimental results. These are the behaviours cited for the current components as a function of both the coordinates ϕ and z.

Next consider the situation, for H-polarization, near the end of the cylinder i.e. $z \lesssim \frac{1}{2}L$. Keep in mind now, however, that the electric field in the incident radiation is primarily parallel to the edge as viewed from the side wall. Actually the amplitude of the component of incident electric field perpendicular to the edge is zero at $\phi=0°$ and $\phi=180°$. It has a cosine type behaviour in between becoming maximum at $\phi=90°$. Thus the effect of any singular type behaviour due to the incident or primary exciting electric field at the edge is certain to be somewhat different than for the E-polarization case. Figure 14 shows that in going from $z=\frac{1}{4}L$ to the circle scanned near the end the component of current $|K_z|$, roughly speaking, changes rather slowly and has actually only a small amplitude. For the remaining distance to the cylinder edge it then continues to decrease to zero at the edge itself. Even this small amplitude component of current displayed some interesting qualitative changes in the azimuthal scans as z goes from $\frac{1}{4}L$ to almost $\frac{1}{2}L$. The component $|K_\phi|$ which blows up at $z=\frac{1}{2}L$ increases, on the average, somewhat as we proceed from $z=\frac{1}{4}L$ to the circle scanned near the end of the cylinder.

From there on out it must rise very rapidly.

Thus far we have only examined the side wall current distributions for E-polarization and for H-polarization. We will next consider the measurements made on the end caps. We begin by pointing out for emphasis these are the only known measurements of this type.

Figures 9 through 11 show the amplitudes of the radial and the azimuthal components of the surface current over the flat end caps for the case of E-polarized incident radiation. To begin with there are some immediate general characteristics evident in all three scans i.e. around a circle of small radius, for $r=\frac{1}{2}a$, and around a circle of radius slightly less than that of the end cap itself. These characteristics are the occurrence of rather low lying minima at $\phi=0°$ and $\phi=180°$ for the azimuthal component of current $|K_\phi|$ accompanied by a marked maximum close to or at the top and bottom of the cap i.e. $\phi=90°$, $\phi= -90°$. Near the cap center this maximum appears just a few degrees toward the illuminated side from $\phi=\pm 90°$. At $r=\frac{1}{2}a$ the maximum shifts toward $\phi=\pm 80°$, i.e. toward the shadow side, as the frequency and hence γ increases. Out near the cap edge we see in figure 11b that this maximum shifts further around the cap toward $\phi=\pm 70°$ on the shadow side as γ increases from 1.068 to 2.136. This of course corresponds to halving the wavelength and keeping the radius and length of the flat capped cylinder fixed. It should also be noted that on the end caps it is somewhat less meaningful to refer to the shadow side or illuminated side. A further property displayed by $|K_\phi|$ in figures 9b through 11b is that the amplitude at the

maximum decreases as γ increases from 1.068 through about γ=1.490. At γ=1.704 the maximum jumps back up and then again decreases as γ increases to 2.136, i.e. double the initial value, except out near the edge of the cap. The second set of γ's always have maxima lying below the first set. Out near $r \approx a$ we see the reversal of these relative heights at the maximum. We point out that at γ=1.704 the closed can is just about one wavelength longer than it is at γ=1.068. What we have been observing is a diffraction characteristic varying with wavelength where the length of the can at γ=1.068 is about $3\lambda/2$ and as γ increases the length also increases until at γ=1.704 it has become $5\lambda/2$. Further increase in γ roughly speaking is basically a repeat of the earlier increase. While $|K_\phi|$ behaves as we have just described we find in figures 9a through 11a the accompanying behaviour of the radial component $|K_r|$ of surface current on the end caps. Maxima occur at ϕ=0° and at ϕ=180° and a minimum at or around ϕ=±90°. This is just the opposite characteristic to that of the $|K_\phi|$ component. Near the center and near the edge of the end cap the principal maxima all occur around on the illuminated side at ϕ=180°. The situation is somewhat more complex halfway out to the edge of the cap. Apparently for the two longer wavelengths the principal maximum occurs back on the shadow side. Otherwise this maximum either occurs on the illuminated side or both the front and back maxima are about equal in height. Near the center of the cap the minimum in $|K_r|$ lies at about ϕ=85° for all frequencies of table 1. Note that this is located toward the shadow

side of the cylinder. At $r=\frac{1}{2}a$ the minimum for $|K_r|$ moves toward the source and for $\gamma=1.068$ it is near $\phi=105°$. As γ increases with decreasing wavelength the minimum moves back away from the source until at $\gamma=1.490$ it is again at about $\phi=80°$. For the larger γ values the minimum stays fixed at about $\phi=85°$ again. Out near the edge there is considerable sensitivity of the location of this minimum in $|K_r|$ with respect to wavelength. At the longest wavelength the minimum appears at about $\phi=55°$. It moves toward the source for $\gamma=1.281$ and appears at $\phi=70°$. For the next two successively larger values of γ it moves back to $\phi=55°$. For $\gamma=1.918$ the $|K_r|$ minimum shifts far around to $\phi=40°$ and for the shortest wavelength $\gamma=2.136$ it again moves back to about 55°. Near the center we have the simple characteristic noted for $|K_\phi|$ at the maximum also displayed for $|K_r|$ at both maxima,namely,the $\gamma=1.068$ maxima are the highest. As γ increases the maxima decrease in relative height. Again at $\gamma=1.704$ these maxima jump back up and then decrease with increasing γ or equivalently with decreasing wavelength. Except for $\gamma=2.136$ the second set lie below the first set. We once again note that the jump occurs when the cylinder effectively becomes one-wavelength longer than the initial length to wavelength ratio. As we move outward toward the edge the variation of this property with wavelength becomes considerably complex and the regularity observed near the cap center is rapidly masked.

Several additional important general features should be also emphasized. First on the end caps we find that the maximum amplitudes of both current components are comparable to those on the

sidewalls near the ends. This is certainly true for the case of E-polarized incident radiation. It should be especially noted that for the longer wavelength radiation the induced currents are, in general, larger. We repeat once again that in the case of E-polarization the incident electric field is oriented normal to the edges of the cylinder and also to the entire flat caps on the ends of the cylinder. Another point to note is that as $r \to o$ we must have $K_\phi(\phi) \to o$ for all ϕ. Judging from figures 9b, and 10b $K_\phi(\phi)$ must fall to zero very rapidly over a very short distance as the center is approached. Similarly, if we are to remain faithful to the conventional wisdom with regard to behaviour at an edge in a three dimensional object, as we approach the edge on the flat end cap we must have $K_r(\phi) \to o$ for all ϕ and $K_\phi(\phi) \to \infty$ for all ϕ. Upon observation of figures 10 and 11 these limits must be attained very rapidly over the short radial distance remaining between that corresponding to figure 11 and the edge itself.

The final sets of data are the end cap azimuthal scans of the amplitudes of the surface current components induced by the incident radiation polarized with the magnetic field parallel to the axis of the cylinder. Azimuthal scans for H-polarization were made over the same circles on the end cap as those in the E-polarization measurements just discussed above. Figures 15 through 17 are the measured azimuthal distributions for the frequencies of Table 1. One immediate observation that can be made is that the $|K_\phi(\phi)|$ distributions for H-polarization have the same general characteristics as the $|K_r(\phi)|$ distributions for E-polarized incident radiation. The major difference

is that the peak heights for $|K_\phi(\phi)|^2$ in figures 15b and 16b are only about one-half those of $|K_r(\phi)|^2$ in figures 9a and 10b for E-polarization. Out near the edge $|K_\phi(\phi)|$ for H-polarization (figure 17b) peaks at about the same height as $|K_r(\phi)|$ for E-polarization (figure 11a). Similar correspondence between $|K_r(\phi)|$ for H-polarization and $|K_\phi(\phi)|$ for E-polarization is evidently displayed. Now however the current component $|K_r(\phi)|^2$ peaks at a height an order of magnitude lower than the peak height of $|K_\phi(\phi)|^2$ for E-polarized incident radiation. The lower values of surface current on the end caps away from the edge of the cap are evidently a consequence of the fact that the electric fields of the incident radiation over the corresponding area is tangent to that area. Also as we pointed out earlier, at the edge itself only a considerably smaller effective incident electric field is normal to the end of the cylinder. The incident field appears to be basically driving surface charge on the sidewall around the cylinder rather than from end to end.

Consider first the behaviour of the azimuthal distribution of $|K_\phi(\phi)|$ as we move from the region near the center of the end cap out toward the edge. If we investigate the location of the minimum, which in all cases is a very low lying point, we observe that near the center of the cap it occurs at about $\phi=\pm 90°$ i.e. at the top and bottom of the scanning circle. At $r=\frac{1}{2}$ a it has shifted quite far around toward the shadow side of the circle of scan and now has located at about $\phi=\pm 65°$. As we move out to the vicinity of the edge of the end cap we find the minimum has moved even further forward to

the neighborhood of $\phi=\pm 40°$. These results are rather different from the E-polarization results at least for $r=\frac{1}{2}a$ and larger scanning circles on the flat end cap. Unlike the E-polarization case the front $\phi=0°$ and back $\phi=180°$ peak heights are about the same in each γ distribution for the small circle of scan near the cap center. At the central scanning circle we find much higher peaks on the illuminated side than on the shadow side. This is true for the whole set of wavelengths. Furthermore we observe that there is a broadening effect at the maximum on the source side of the cap. In addition we note that near $\phi=0°$ the highest peak is that for the longest wavelength, $\gamma=1.068$. As γ increases, and the wavelength decreases the peak height drops. Again as the effective length changes by a wavelength at $\gamma=1.704$ the peak height jumps back up and then decreases with further increase in γ. Near $\phi=180°$ this behaviour again recurs although the maximum peak height now corresponds to $\gamma=1.704$. Roughly similar behaviour is displayed at the small inner scanning circle. There however the $\gamma=1.281$ peak sits above the $\gamma=1.068$ peak at $\phi=0°$ and $\phi=180°$. At the outermost scanning circle this ordering becomes considerably different. The shorter wavelengths seem to correspond to the higher peaks out near the edge. Now we can easily see a rather extensive broadening of the high current region from about $\phi=80°$ to $\phi=180°$. This is a rather striking behaviour and contrasts somewhat vividly when compared with $|K_\phi(\phi)|$ for the E-polarization results. Note that the amplitudes are comparable for both polarizations out near the edge. For H-polarization there is an evident increase in the average value of

$|K_\phi(\phi)|$ as $r \to a$. Again if $K_\phi(\phi)$ is to become infinite at r=a it will have to increase at an immense rate as the remaining short distance to the edge is traversed. One last point with regard to the azimuthal component of current. If we compare figure 14b for this quantity on the sidewall near the end cap we observe a most remarkable similarity with the distribution for $|K_\phi(\phi)|$ in figure 17b on the end cap near the edge.

For H-polarized incident radiation we note that the amplitude distribution of the radial component of surface current over the end cap is qualitatively similar to the $|K_\phi|$ distribution for E-polarized incident radiation. Again a major difference lies in the H-polarized case showing $|K_r(\phi)|^2$ to be an order of magnitude lower than the $|K_\phi(\phi)|^2$ for the E-polarized case. On the small inner scanning circle we find in figure 15b the peak in the amplitude of the radial component of current is at about $\phi=\pm 60°$ for the longest wavelength case, $\gamma=1.068$. It moves toward the source lying at $\phi=\pm 90°$ when $\gamma=1.281$ and then moves back to $\phi=\pm 80°$ as the wavelength decreases to $\gamma=1.490$. Further decreasing the wavelength shifts this peak to $\phi=\pm 100°$ and again back to $\phi=\pm 90°$ at the shortest wavelength, $\gamma=2.136$. This behaviour is quite different from that found for $|K_\phi(\phi)|$ at E-polarization as seen in figure 9a. At the central scanning circle this shifting back and forth of the peak with increasing frequency is again observed. Here the longest wavelength incident radiation $\gamma=1.068$ results in the peak lying at about $\phi=\pm 95°$. For $\gamma=1.281$ the peak shifts to $\phi=\pm 80°$. At $\gamma=1.490$ the peak shifts in the opposite direction to $\phi=\pm 100°$. For the next two shorter wavelengths it moves

way back to about $\phi=\pm 55°$ and finally again moves slightly toward the source so that for $\gamma=2.136$ it lies at about $\phi=\pm 60°$. This behaviour again occurs on the outermost scanning circle. For the three longest wavelengths the peak lies at about $\phi=\pm 80°$. At $\gamma=1.704$ it moves to $\phi=\pm 60°$. For $\gamma=1.918$ it is at $\phi=\pm 120°$ and finally at the shortest wavelength it returns again to $\phi=\pm 80°$. We thus observe a range of about 45° for the location of the maximum of $|K_r(\phi)|$ in the H-polarization case. This is about twice the range for $|K_\phi(\phi)|$ in the E-polarization case. It is very likely that this difference is basically the result of the relative effective E-fields normal to the edge, both with respect to amplitude and direction in the two cases of E-polarized incident radiation and H-polarized incident radiation. Near the center of the cap the longer wavelengths give rise to the higher maxima for $|K_r(\phi)|$ although there is no great difference in the peak heights. At the $r=\frac{1}{2}a$ circle of scan this again is nearly the case. Here the largest peak is that for $\gamma=1.704$. This is followed by the peak for the two longest wavelengths. However the third longest wavelength radiation results in the next to lowest peak height for the distribution around the middle of the end cap. Near the edge of the end cap $\gamma=1.704$ again produces the highest peak in $|K_r(\phi)|$. This is again followed by the peak for $\gamma=1.068$. Further decreasing the wavelength does not result in an easily discerned ordering of the resultant peak height for the induced radial component of current. It should also be noted that the peaks in figures 15a, 16a and 17a in $|K_r(\phi)|^2$ are all about as

high as the minima for $|K_\phi(\phi)|^2$ in figures 15b, 16b and 17b. Also comparing $|K_r(\phi)|^2$ near the edge of the end cap (figure 17a) with $|K_z(\phi)|^2$ on the sidewall near the end of the cylinder we find that very roughly the former are somewhat larger in amplitude than the latter. It is not too difficult to assume that the radial component distribution may indeed fall to zero for all ϕ as $r \to a$.

We have now discussed in some detail the experimentally observed behaviour of the distribution of the amplitudes of the surface current components on the flat-capped cylinder. This has been done as a function of wavelength for both E-polarized and H-polarized incident radiation. What we have found is a rather complex response of the cylinder to the incident electromagnetic radiation. Nevertheless a remarkable degree of orderly behaviour can be deduced from the experimental data. In the next section, we shall summarize our results for this problem and there add to the observations already made above.

IV. SUMMARY DISCUSSION OF THE DIFFRACTION PROBLEM

As we pointed out in reviewing the history of the problem of diffraction of electromagnetic radiation by a finite length, conducting circular cylinder, flat-capped at both ends, there appears to be no theoretical solution--neither analytic nor numerical--for the situation when the wavelength of the incident radiation is comparable to both the length and the diameter of the cylinder. The extensive literature on cylinders, both near-field and far-field investigations, seems to be devoid of experimental and theoretical results for the system reported on in this paper. Since this is a three-dimensional non-spherical system which approximates, more or less, many real systems we have helped to fill a gap in knowledge relative to a class of electromagnetic diffraction and scattering problems that are of considerable practical importance. It should be emphasized that in this study neither of the two essential parameters, circumference to wavelength ratio, and length to wavelength ratio are asymptotic in any sense.

The detailed experimental results for the distributions of the amplitudes of the components of induced surface current on the sidewall and the flat end-caps of the conducting cylinder and the variation of these distributions with wavelength and polarization of the incident radiation are not only of importance in giving us the characteristic response of the capped cylinder. This, of course, implies that we now have a corresponding insight into how such incident radiation will induce currents over the surface of many

real but more complex systems which can be approximately modeled by such a simple geometry. What is of equal, if not greater, importance when we investigate the field and current distributions for similar systems which contain apertures we shall be able to understand in detail how such apertures and their intrinsic parameters affect and modify the fields and surface currents of the closed cylindrical can. This in turn leads to an understanding of the response of a much larger class of highly important real systems when similarly irradiated. One result of such knowledge is we shall then possess the capability of modifying the design of real complex systems to either enhance or reduce one or more effects. To develop this capability for pulsed incident radiation we are now in a position to proceed in a semi-empirical approximate fashion. By appending to the type of experimental data obtained and presented in this report approximate analytic asymptotic solutions for one or the other basic parameters we shall have the response for all frequencies. Utilizing the available repertoire of Fourier inversion techniques we can then obtain considerable, although still approximate, knowledge of the response of many systems to pulsed radiation.

In examining the details of the measured induced surface current distributions we have already highlighted a number of important properties they displayed. As an example of these we have indicated when the infinite circular cylinder results can be safely used to describe corresponding phyiscal quantities for the finite length, capped cylinder. This property together with the symmetry observed in the measurements leads to a remarkable degree of insight for

analytically resolving the diffraction problem either formally or numerically. It should be noted that prior to these measurements such guidance either was non-existent or else rested on a very shaky foundation. It should be remembered that the measured distributions are actually a solution in themselves. Nevertheless it is highly desirable to achieve analytic solution of the problem also as this more often than not leads to a greater area of understanding of similar problems. With the sets of measurements as one starting point it should not be too far in the future before an appropriate complete formal analytic solution can be obtained. We have already moved quite a way toward achieving this end and shall present our results in a forthcoming publication. One point that was raised in the course of examining the data in this paper is the question of the behaviour of fields and currents in the vicinity of sharp edges. As we have indicated above many outstanding attempts have been made to understand such edge effects. They all have one common characteristic, namely, they assume that the behaviour at an edge on a finite three-dimensional object is basically the same as that for a two dimensional one. The argument presumes that the properties at a point on such an edge depends only on the local properties of nearby fields and currents. It should be noted that for our finite cylinder we have another edge not too teribly far away and the precise role it plays in the currents and fields at the edge in question is not very clear. Nevertheless, we have developed an analytical tool that can address itself specifically to such problems and the results of applying it to resolve the question cited

shall be reported on in a later paper.

This paper is the first in a series of reports on extensive measurements made for finite circular conducting cylinders. Following this report we shall present experimental results for cylinders with apertures of varying characteristics. These subsequent publications will occasionally be semi-empirical studies. In each case we shall see that the discussion of the results reveals properties that shed considerable light on how to obtain analytic solution of the corresponding problem.

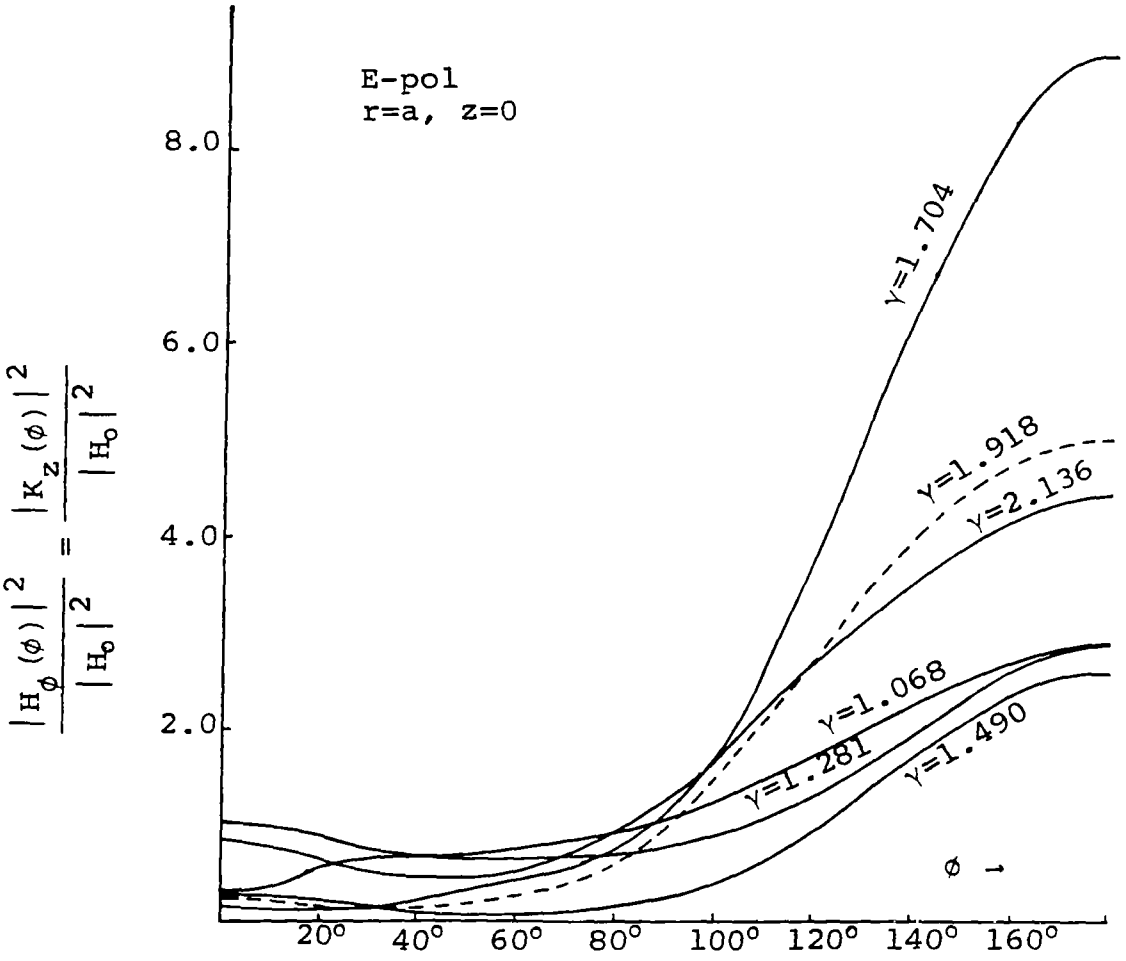

Figure 6. Azimuthal Scans of Amplitude of Longitudinal Component of Surface Current Around Center of Flat Capped Conducting Cylinder of Length=46 cm and Radius=5.10 cm.

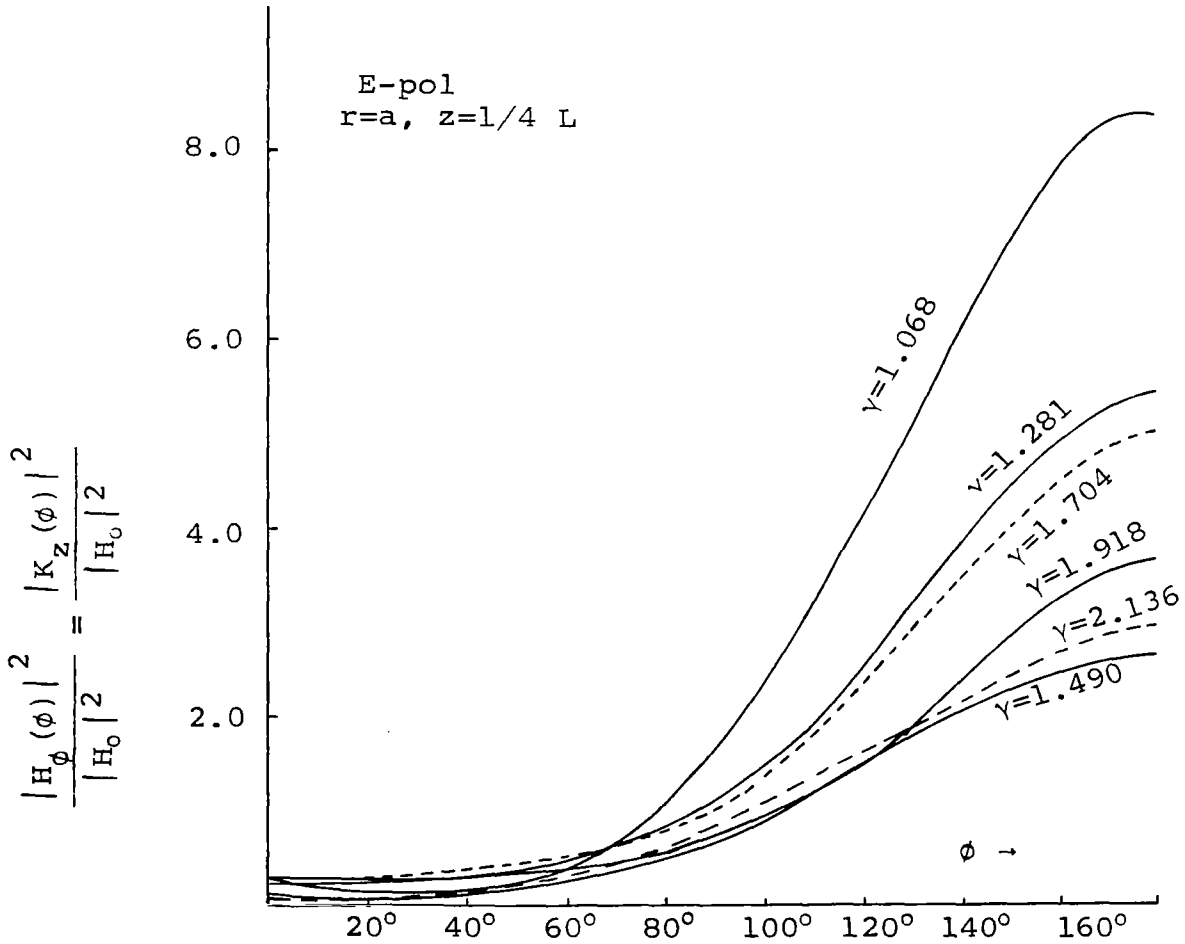

Figure 7. Azimuthal Scans of Amplitude of Longitudinal Component of Surface Current Halfway Between Center and End of Flat Capped Conducting Cylinder of Length=46 cm and Radius=5.10 cm.

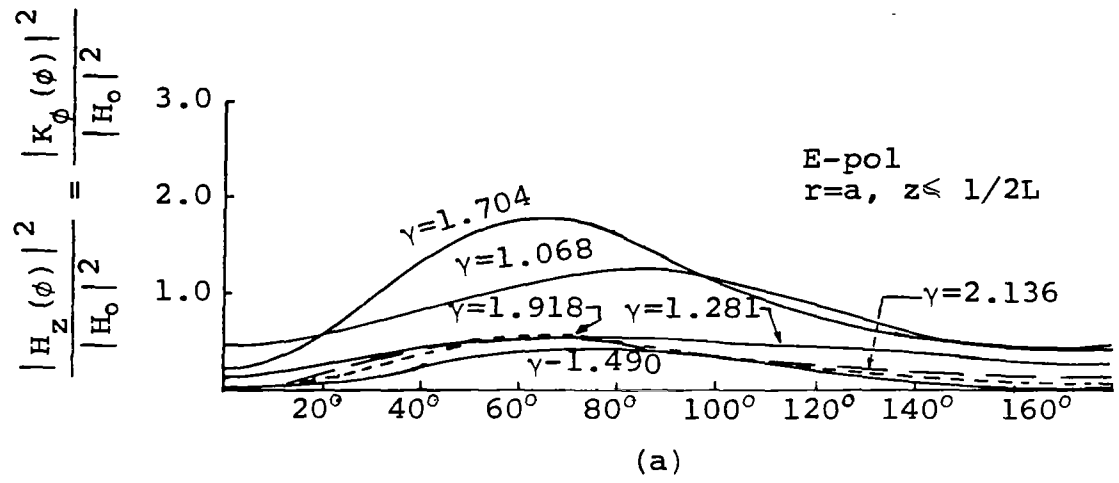

(a)

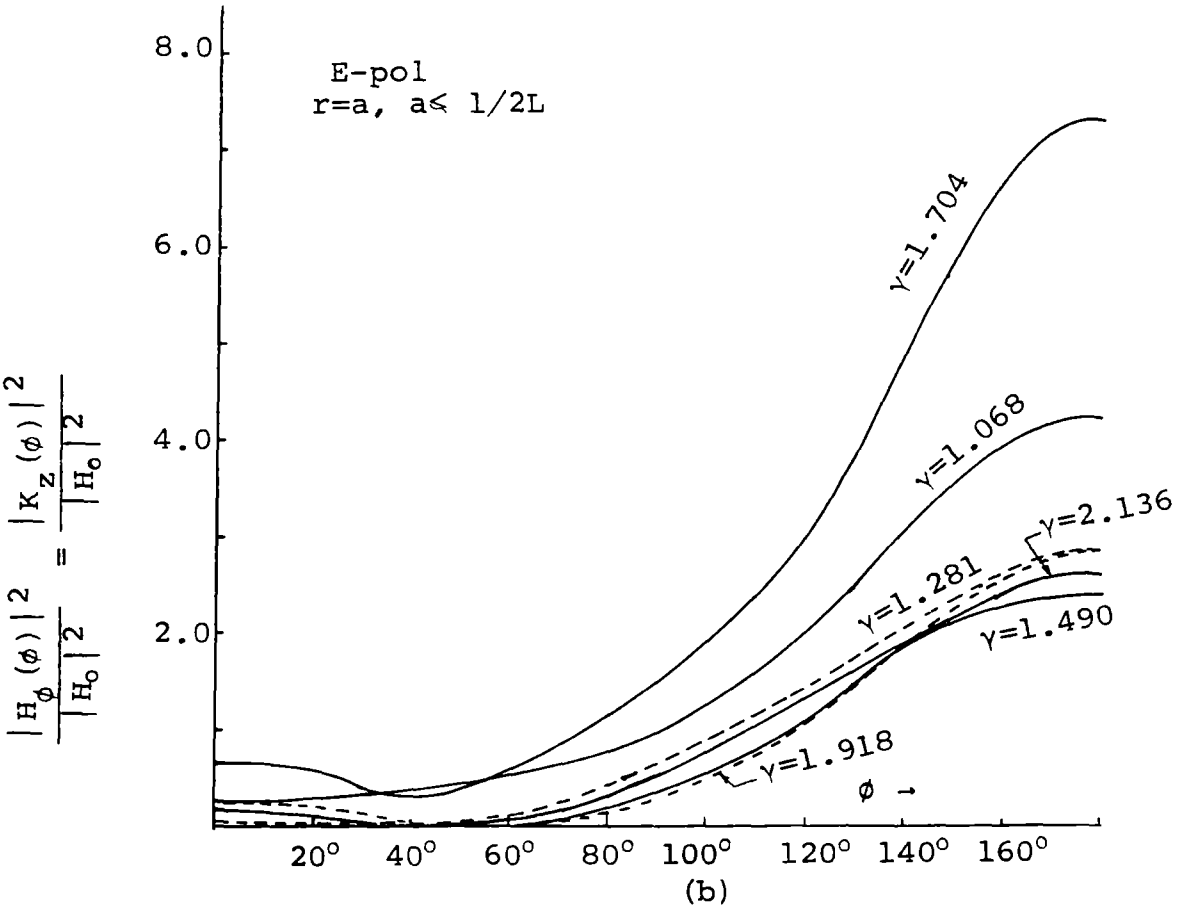

(b)

Figure 8. Azimuthal Scans of Amplitude of Azimuthal Component (a) and Longitudinal Component (b) of Surface Current Near End of Flat Capped Conducting Cylinder of Length=46 cm and Radius=5.10 cm.

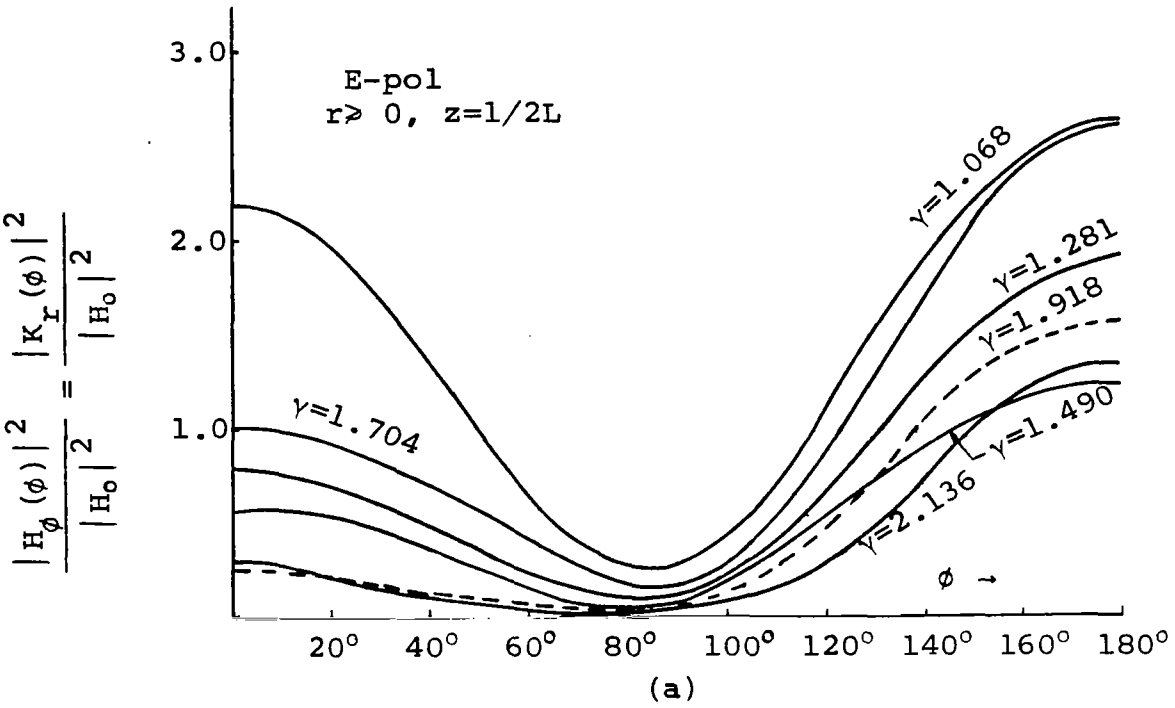

(a)

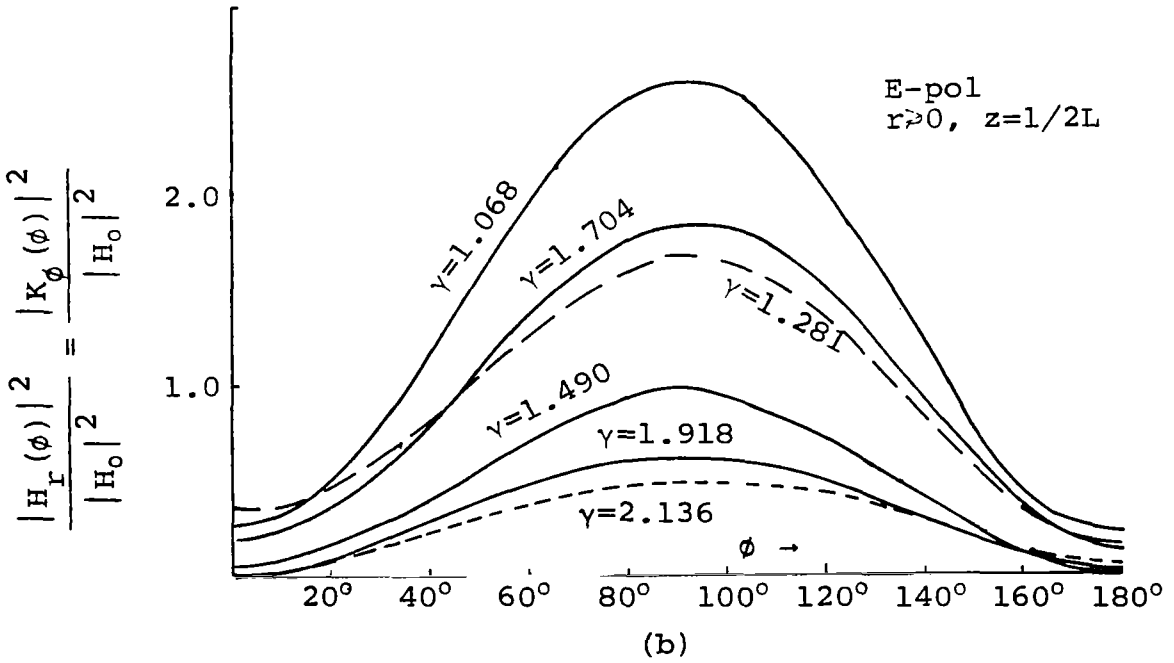

(b)

Figure 9. Azimuthal Scans of Amplitude of Radial Component (a) and Azimuthal Component (b) of Surface Current Near Center of End Cap of Conducting Cylinder of Length L=46 cm and Radius a=5.10 cm.

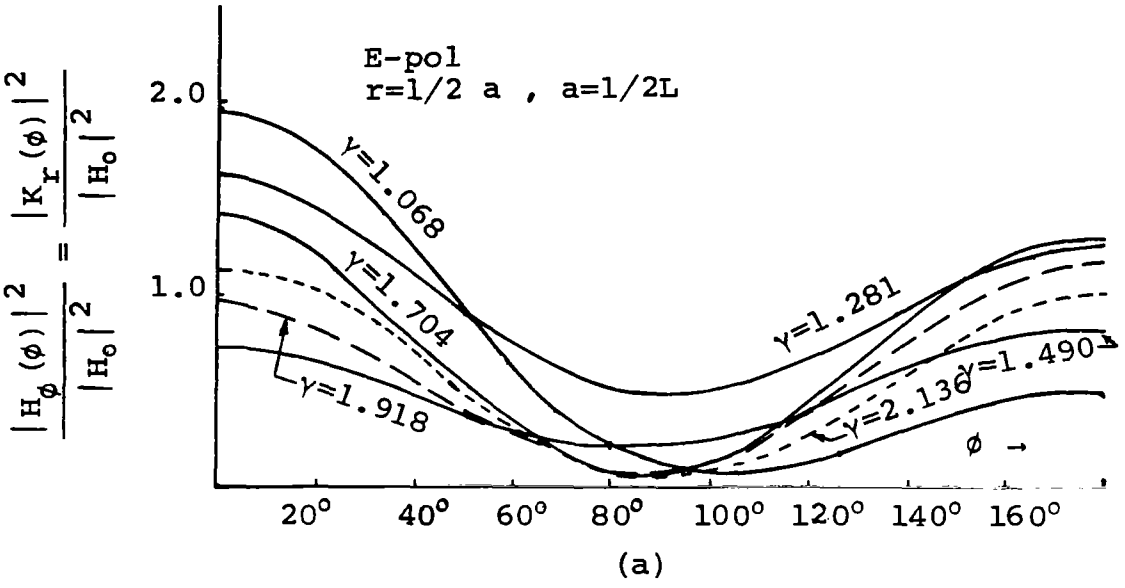

(a)

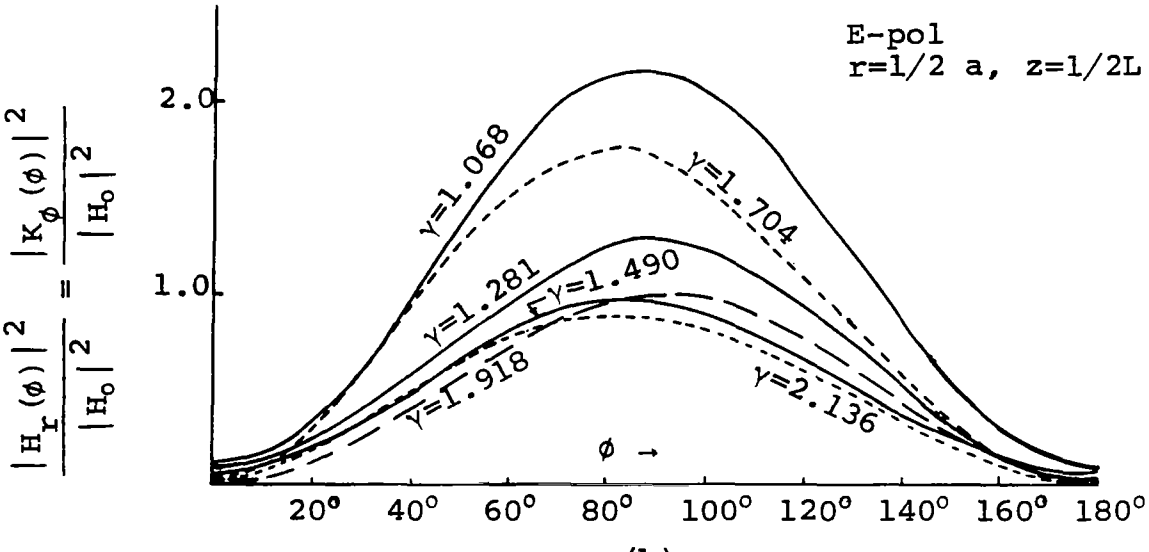

(b)

Figure 10. Azimuthal Scans of Amplitude of Radial Component (a) and Azimuthal Component (b) of Surface Current at r=1/2a on Flat End Cap of Conducting Cylinder of Length=46 cm and Radius=5.10 cm.

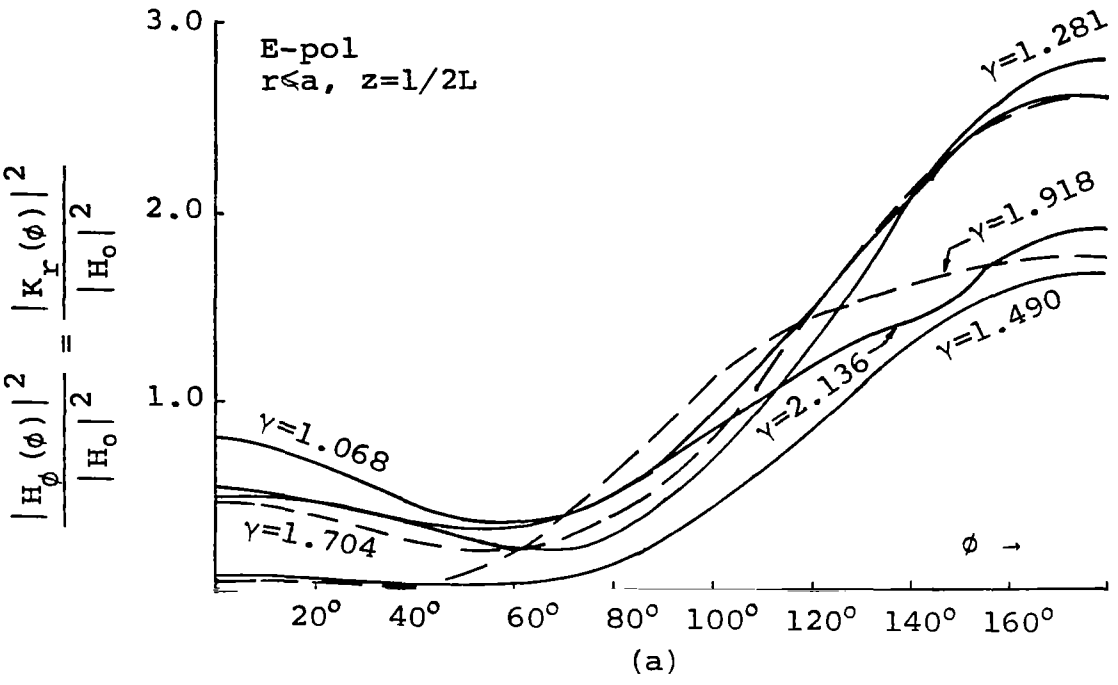

(a)

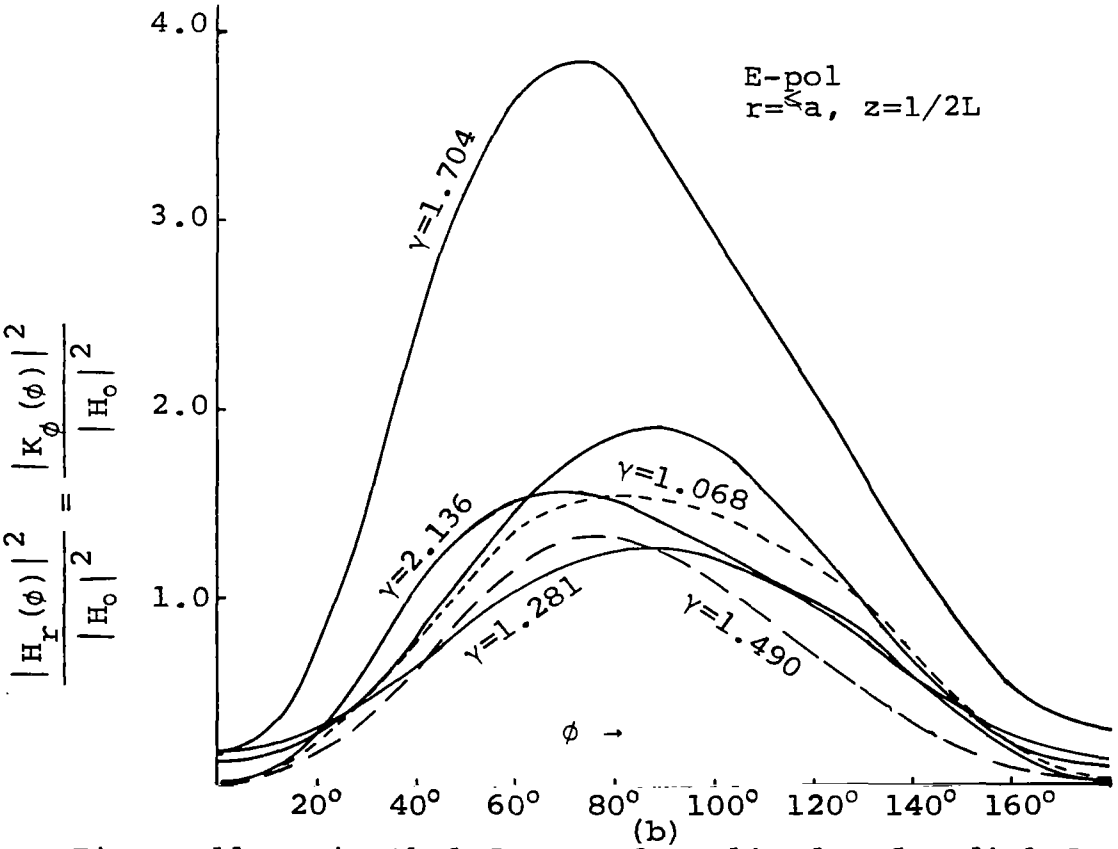

(b)

Figure 11. Azimuthal Scans of Amplitude of Radial Component (a) and Azimuthal Component (b) of Surface Current Near Edge of Flat End Cap of Conducting Cylinder of Length=46 cm and Radius=5.10 cm.

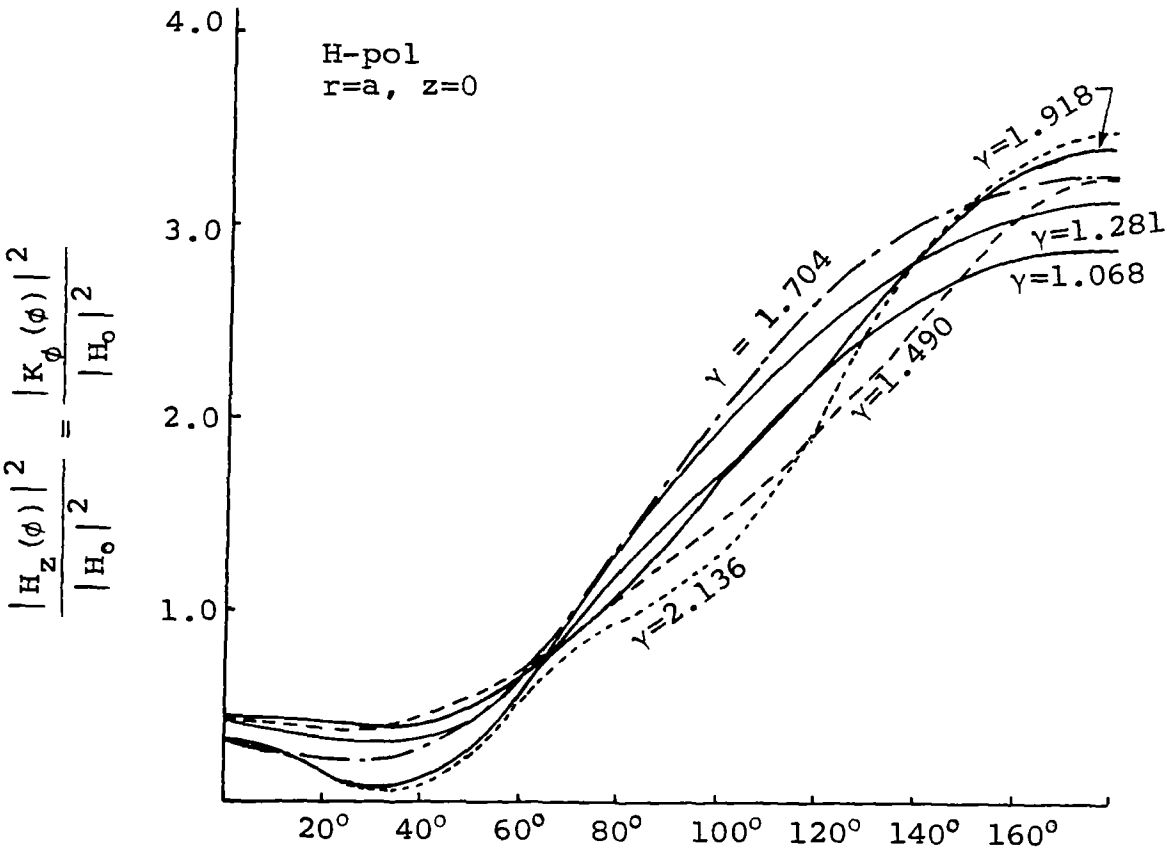

Figure 12. Azimuthal Scans of Amplitude of Azimuthal Component of Surface Current Around Center of Flat Capped Conducting Cylinder of Length=46 cm and Radius=5.10 cm.

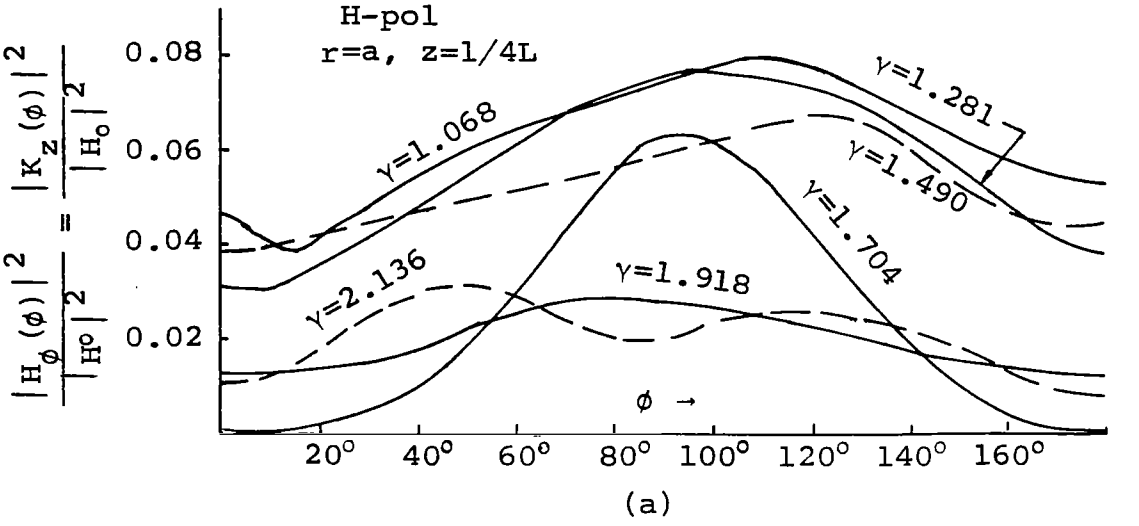

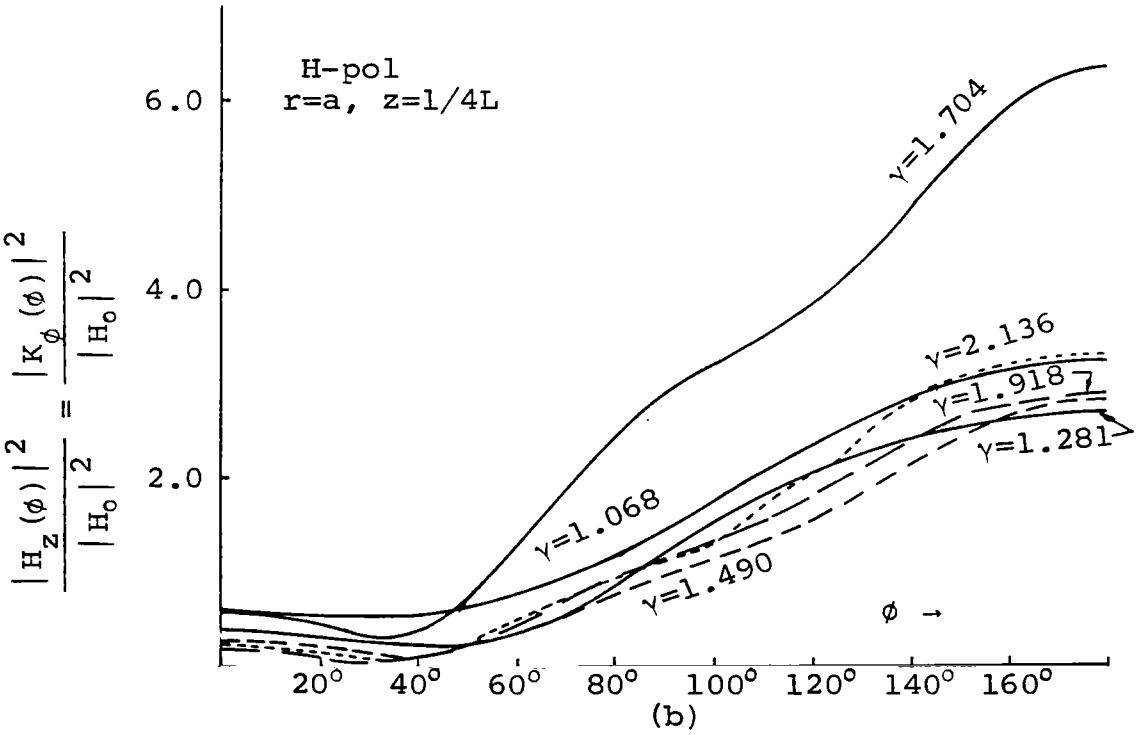

Figure 13. Azimuthal Scans of Amplitude of Longitudinal Component (a) and Azimuthal Component (b) of Surface Current Halfway between Center and End of Flat Capped Conducting Cylinder of Length=46 cm and Radius 5.10 cm.

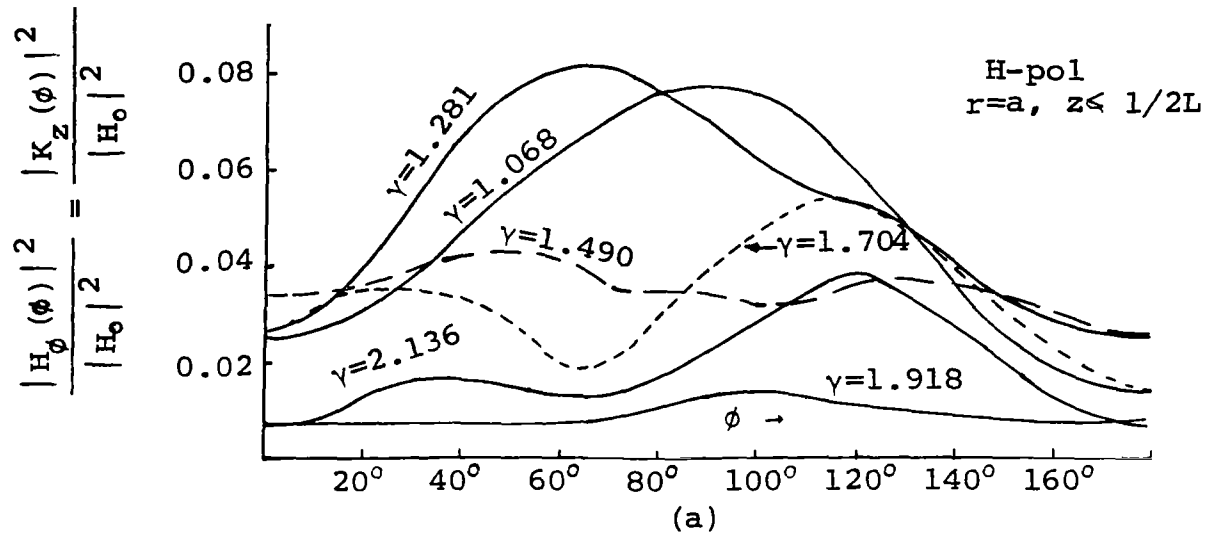

(a)

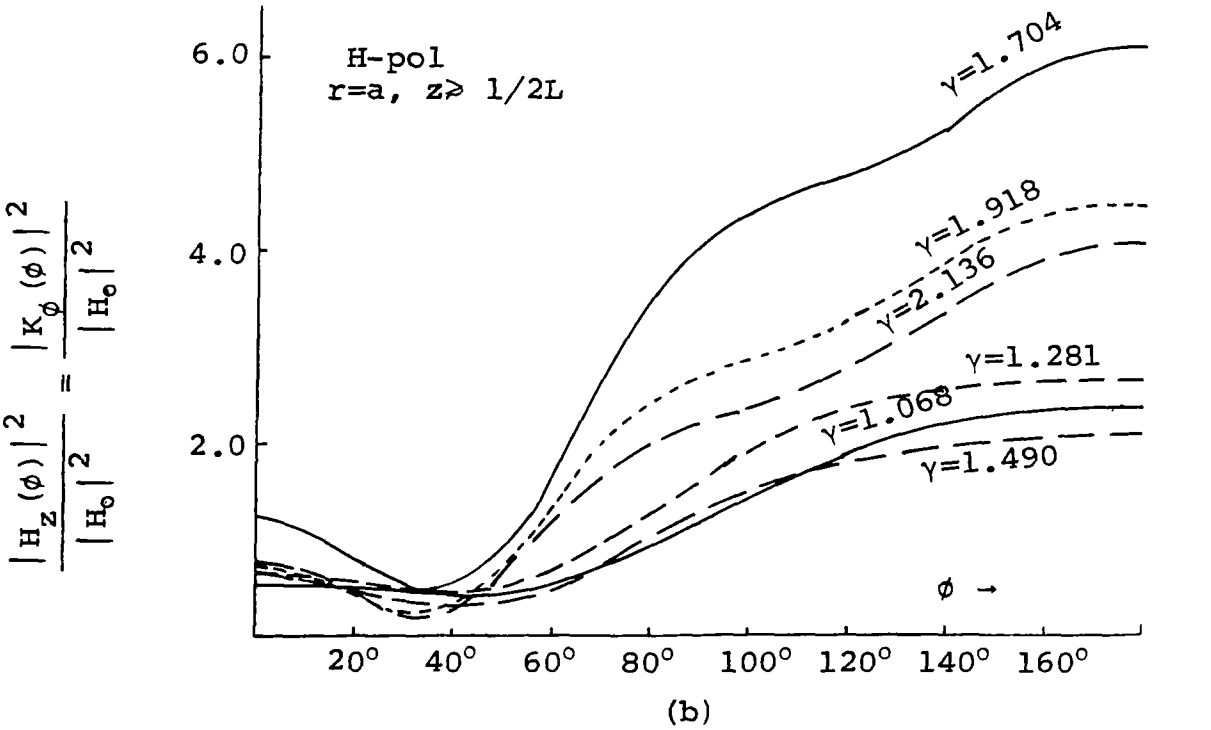

(b)

Figure 14. Azimuthal Scans of Amplitude of Longitudinal Component (a) and Azimuthal Component (b) of Surface Current Near End of Flat Capped Conducting Cylinder of Length=46 cm and Radius=5.10 cm.

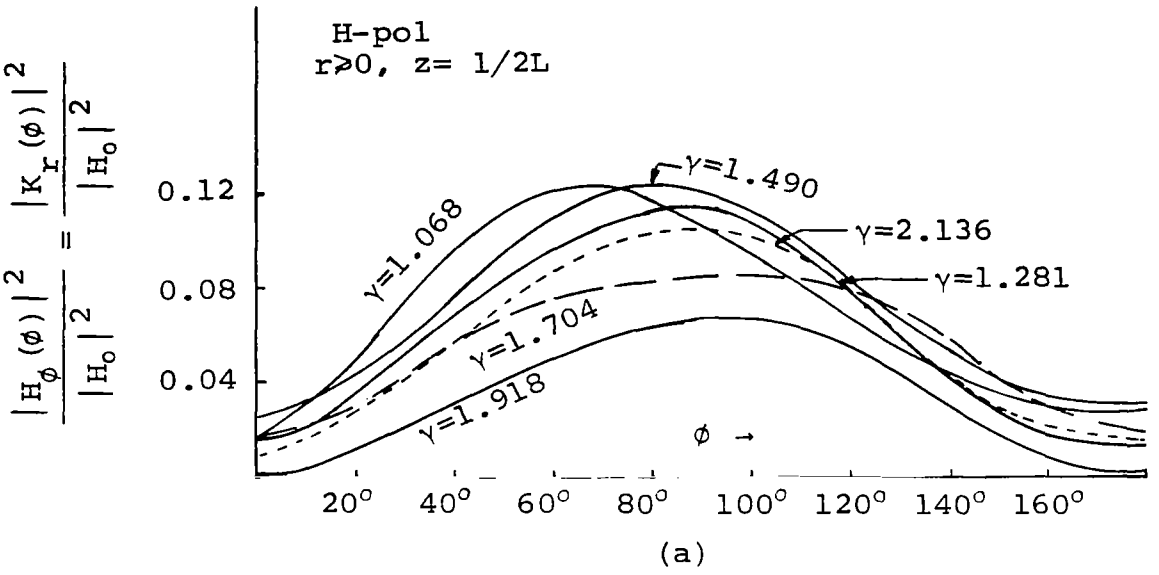

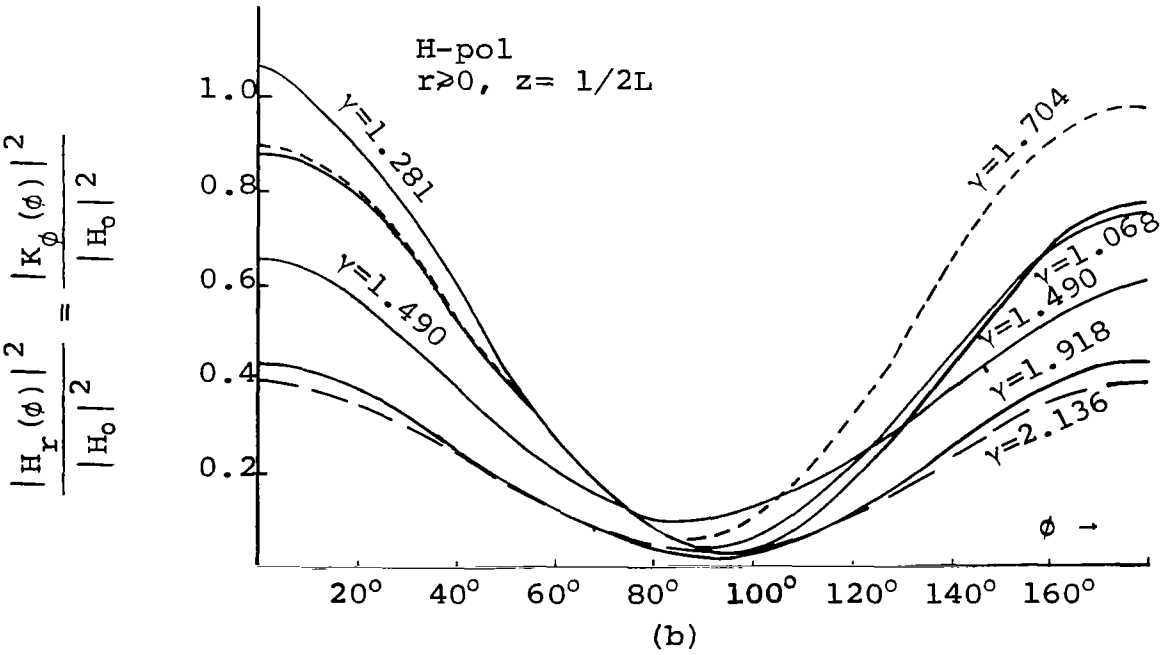

Figure 15. Azimuthal Scans of the Amplitude of the Radial Component (a) and the Azimuthal Component (b) of Surface Current Near Center of End Cap of Conducting Cylinder of Length=46cm and Radius=5.10 cm.

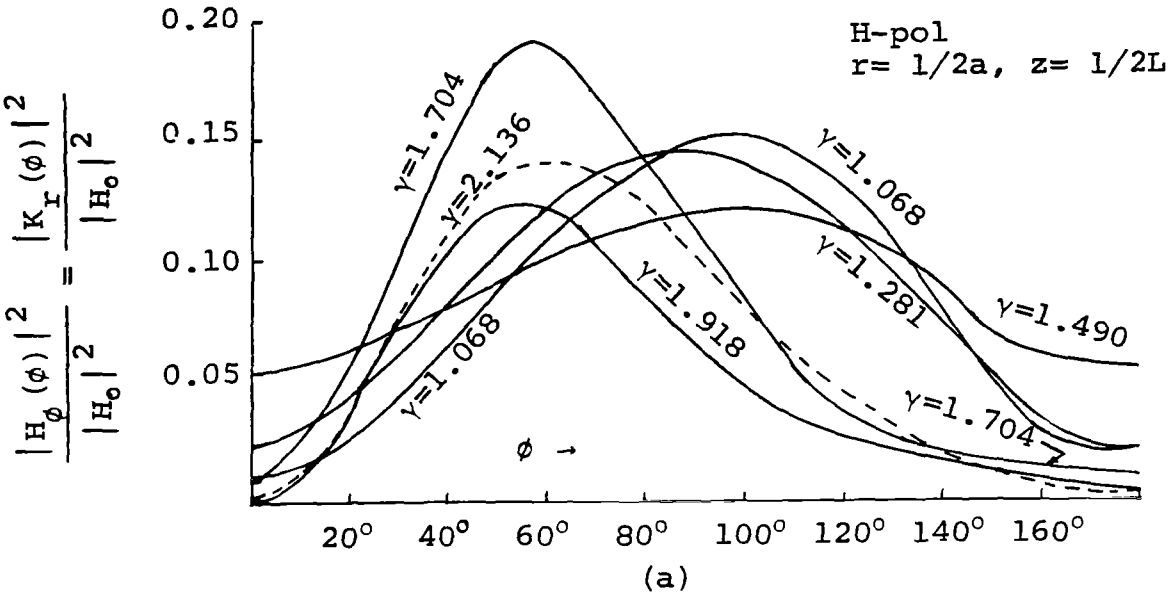

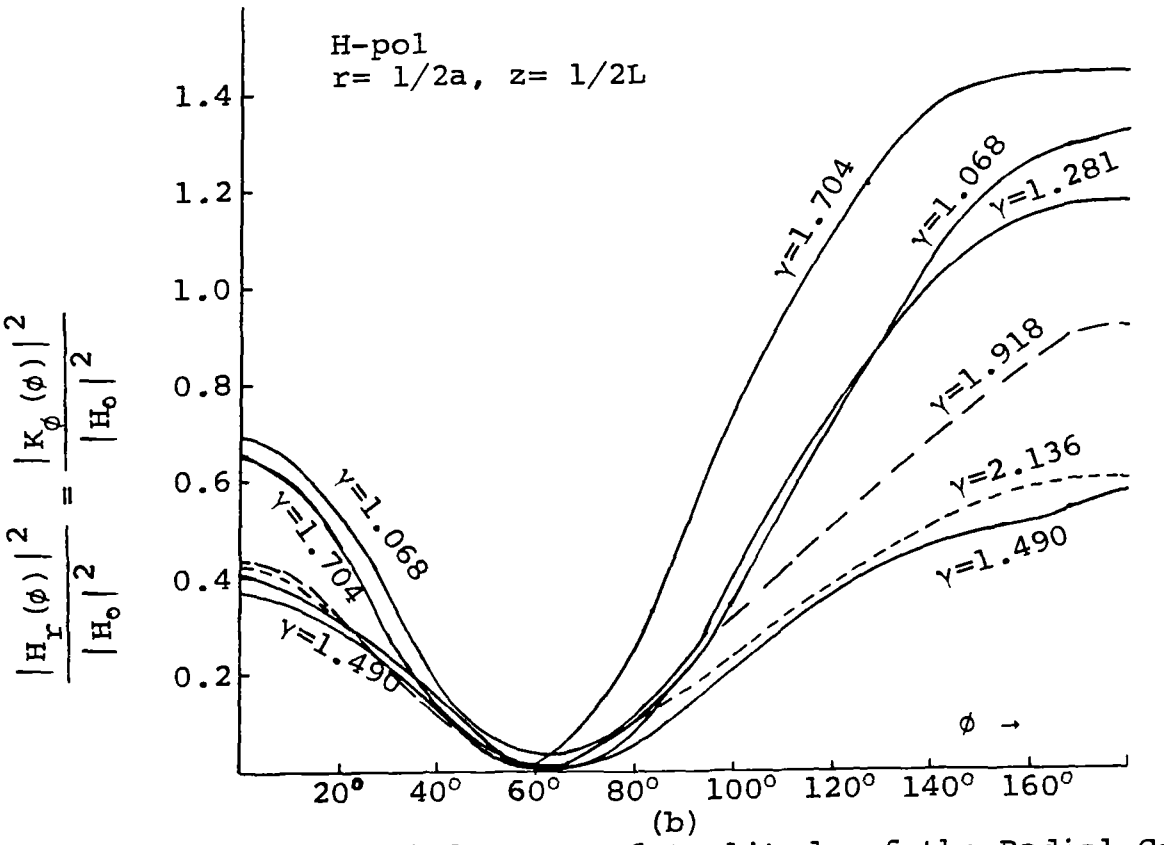

Figure 16. Azimuthal Scans of Amplitude of the Radial Component(a) and the Azimuthal Component (b) of the Surface Current at r=1/2a on Flat End Cap of Conducting Cylinder of Length=46cm and Radius= 5.10 cm.

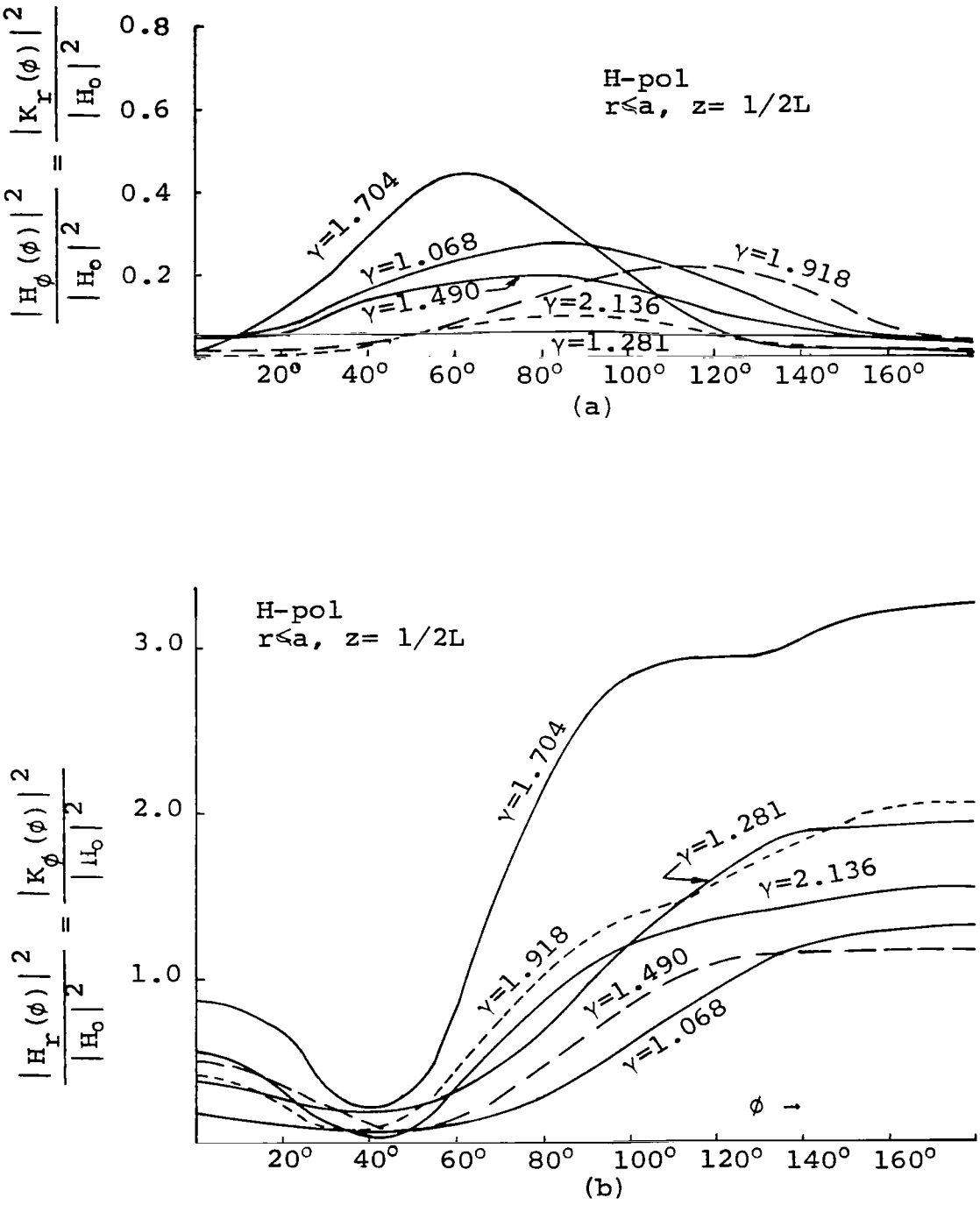

Figure 17. Azimuthal Scans of the Amplitude of the Radial Component (a) and the Azimuthal Component (b) of Surface Near the Edge of the Flat End Cap of the Conducting Cylinder of Length=46 cm and Radius=5.10 cm.

REFERENCES

1. A. W. Maue, "Zur Formulierung eines Allgemeinen Beugungsproblems durch eine Integralgleichung," Zeitschrift für Physik 601, 126 (1949).

2. H. Hönl, A. W. Maue, K. Westpfahl, "Theorie der Beugung," Vol. XXV/1 pp. 311, 354-362, Handbuch der Physik, Springer-Verlag, Berlin, 1961.

3. J. Van Bladel, "Electromagnetic Fields," p. 354, McGraw-Hill Book Co., N.Y., 1964.

4. C. J. Bouwkamp, "A Note on Singularities At Sharp Edges In Electromagnetic Theory," Physica, 467-474, 12 (1946).

5. J. Meixner, Die Kantenbedingung in der Theorie der Beugung Electromagnetisher Wellen an Vollkommen Leitenden Ebenen Schirmen," Ann. Physik, 2-9, 441 (1949).

6. J. Meixner, "The Behaviour of Electromagnetic Fields at Edges," N.Y.U. Inst. Math, Sci. Res. Rept. EM-72, December 1954.

7. D. S. Jones, "Note on Diffraction by An Edge," Quart. J. Mech. and Appl. Math 420, 3 (1950).

8. A. E. Heins, S. Silver, "The Edge Condition and Field Representation Theorems In the Theory of Electromagnetic Diffraction," Proc. Camb. Phil. Soc. 149, 51 (1955).

9. D. S. Jones, Section 9.1, "The Theory of Electromagnetism," MacMillan Co., New York, N.Y. 1964.

10. R. E. Collins, F. J. Zucker, Section 1.7, "Antenna Theory" Part I, McGraw-Hill Book Co., New York, N.Y. 1969.

11. D. Greenspan, P. Werner, "A Numerical Method for The Exterior Dirichlet Problem for the Reduced Wave Equation," Arch. Ration. Mech. Anal., 288, 23 (1966).

12. P. R. Garabedian, "An Integral Equation Governing Electromagnetic Waves," Quart. Appl. Math., 428, 12 (1955).

13. P. C. Waterman, "Matrix Formulation of Electromagnetic Scattering," Proc. IEEE, 805, 53, Aug 1965.

14. H. A. Schenk, "Improved Integral Equation Formulation For Acoustic Radiation Problem," Acoust. Soc. Am., 41, 44 (1968).

15. K. M. Mitzner, "Numerical Solution of the Exterior Scattering Problem at Eigen Frequencies of The Interior Problem," 1968, U.R.S.I. Meeting, Boston, Mass. March 1968.

REFERENCES (Contd.)

16. H. Brakhage, P. Werner, "Über des Dirichletsche Aussenraumproblem für die Helmholtzsche Schwingungsgleichung," Arch. Math. Chapter 16, pp. 325-329 (1965).

17. J. C. Bolomey, W. Tabbara, "Numerical Aspects on Coupling Between Complementary Boundary Value Problems," IEEE Trans. on Ant. and Propag. 356, AP-21 (1973).

18. J. C. Bolomey, W. Tabbara, "Sur la Resolution Numerique de l'Equation des Ondes pour des Problemes Complementaires," C. R. Acad. Sci. (Paris), 933, 271B (1970).

19. J. C. Bolomey, W. Tabbara, "Influence du Mode de Representation de l'Onde Diffractee Sur la Resolution Numerique d'un Probleme de Diffraction," C. R. Acad. Sci. (Paris), 1001, 270B (1970).

20. J. C. Bolomey, These d'Etat Université de Paris XI, Paris, France May 1971.

21. R. F. Kussmaul and P. Werner, "Fehlerabschätzungen für ein Numerisches Verfahren zur Auflösung Linearer Integralgleichungen mit Schwachsingulärer Kerner," Comput. Jour. 22, 3 (1968).

22. J. H. VanVleck, F. Bloch, M. Hammermesh, "Theory of Radar Reflection from Wires and Thin Metallic Strips," Jour. Appl. Phys. 274, 18 (1947).

23. F. Bloch, M. Hammermesh, Technical Memo 411-125 of the Radio Research Laboratory, Harvard University, Cambridge, Mass., June 20, 1944.

24. E. Siegal, J. Labus, Hoch: tech. und Elek:akus., 166, 43 (1934).

25. E. Hallén, "Theoretical Investigations into the Transmitting and Receiving Qualities of Antennae," Nova Acta Reg. Soc. Scient. Upsaliensis, 1, 11 (1938).

26. E. Hallén, "Exact Treatment of Current Wave Reflection at the End of a Tube Shaped Cylindrical Antenna," I.R.E. Trans. on Ant. and Propag. 479, AP-4 (1956).

27. E. Hallén, "Exact Solution of the Antenna Equation," Electromagnetic Theory and Antennas, Ed. E. C. Jordan, Pergamon Press, New York, p. 1131, 1963.

28. R. King, C. W. Harrison, Jr., "The Distribution of Current Along A Symmetrical Center-Driven Antenna," Proc. I.R.E. 548, 31 (1943).

REFERENCES (Contd.)

29. R. King, C. W. Harrison, Jr., "The Receiving Antenna," Proceedings of I.R.E., 18, 32 (1944).

30. R. King, C. W. Harrison, Jr., "The Receiving Antenna In a Plane-Polarized Field of Arbitrary Orientation," Proc. I.R.E. 35, 32 (1944).

31. M. C. Gray, "A Modification of Halléns Solution of the Antenna Problem," Jour. Appl. Phys. 61, 15 (1944).

32. R. King, D. Middleton, "The Cylindrical Antenna: Current and Impedance," Quart. Appl. Math, 302, 3 (1946).

33. D. Middleton, R. King, "The Thin Cylindrical Antenna: A Comparison of Theories," Jour. Appl. Phys. 273, 17 (1946).

34. R. B. Kieburz, "Scattering by a Finite Cylinder," Electromagnetic Waves, Ed. E. C. Jordan, Pergamon Press, New York, p. 145, 1963.

35. C. Flammer, "Equivalent Radii of Thin Cylindrical Antennas With Arbitrary Cross Sections," Stanford Research Inst. Tech. Rep. 4, 1950, Stanford, Calif.

36. C. W. H. Su, J. P. German, "The Equivalent Radius of Noncircular Antennas," Microwave Jour. 64, 9 (1966).

37. S. Uda, Y. Mushiake, Yagi-Uda Antenna, Sasaki Printing and Publishing Co. Ltd., Sendai, Japan 1954.

38. C. T. Tai, "Radar Response From Thin Wires," Stanford Res. Inst. Tech. Rep. 18, Stanford, Calif. 1951.

39. C. T. Tai, "Electromagnetic Back-Scattering From Cylindrical Wires," Jour. Appl. Phys. 909, 23 (1952).

40. G. T. Ruck, D. E. Barrick, W. D. Stuart, C. K. Krichbaum, "Radar Cross-Section Handbook," Vol. 1, Plenum Press, N.Y. Section 4.3.2.2, 1970.

41. A. I. Carswell, "Microwave Scattering Measurements in the Rayleigh Region Using a Focused-Beam System," Canad. Jour. of Phys. 1962, 43 (1965).

42. C. L. Andrews, "Diffraction of Microwaves Near Rods," Jour. Appl. Phys. 465, 22 (1951).

REFERENCES (Contd.)

43. A. C. Lind, "Resonance Electromagnetic Scattering by Finite Circular Cylinders," Ph.D. Dissertation, Rensselaer Polytechnic Institute, Troy, New York 1966.

44. R. F. Harrington, J. R. Mautz, "Straight Wires With Arbitrary Excitation and Loading," IEEE Trans. on Antennas and Prop., 502, AP15 (1967).

45. J. H. Richmond, "Digital Computer Solutions of the Rigorous Equations for Scattering Problems," Proc. of IEEE, 796, 53 (1965).

46. R. Dell, C. Carpenter and C. L. Andrews, Jour. Opt. Soc. of Am. 62, 902 (1972).

47. L. F. Libelo, J. P. Heckl, C. L. Andrews, D. P. Margolis, 1975 IEEE International EMC Symposium, October 1975, San Antonio, Texas, Paper No. 5BI.

48. D. P. Margolis, Ph.D. Dissertation, State University of New York at Albany. Albany, N.Y. January 1976.

49. D. P. Margolis, C. L. Andrews, R. L. Kligman, L. F.Libelo, Bull. Amer. Phys. Soc., 456, 19 April 1974.

50. J. J. Bowman, T.B.A. Senior and P.L.E. Uslenghi, eds., "Electromagnetic and Acoustic Scattering by Simple Shapes," Chapt. 2, North Holland Publishing Co., Amsterdam, The Netherlands 1969.

51. R. F. Harrington, "Time Harmonic Electromagnetic Fields," p. 232-234 McGraw-Hill Book Co., New York 1961.

52. M. Kerker, "The Scattering of Light and Other Electromagnetic Radiation," Chapt. 6, Academic Press, New York 1969.

53. R.W.P. King, T.T. Wu, "The Scattering and Diffraction of Waves," Harvard Univ. Press, Cambridge, Mass. 1959.